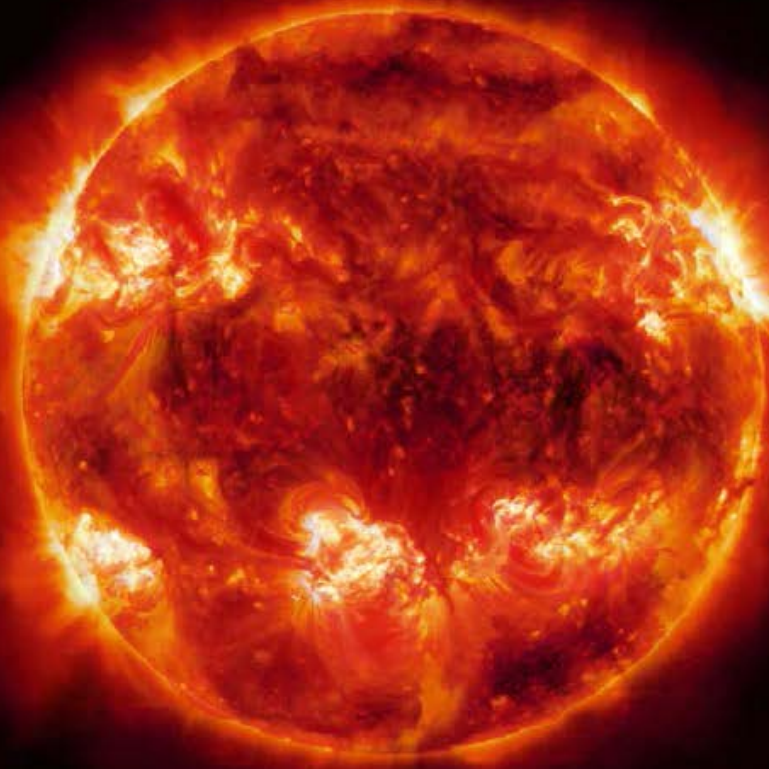


Photons in the universe

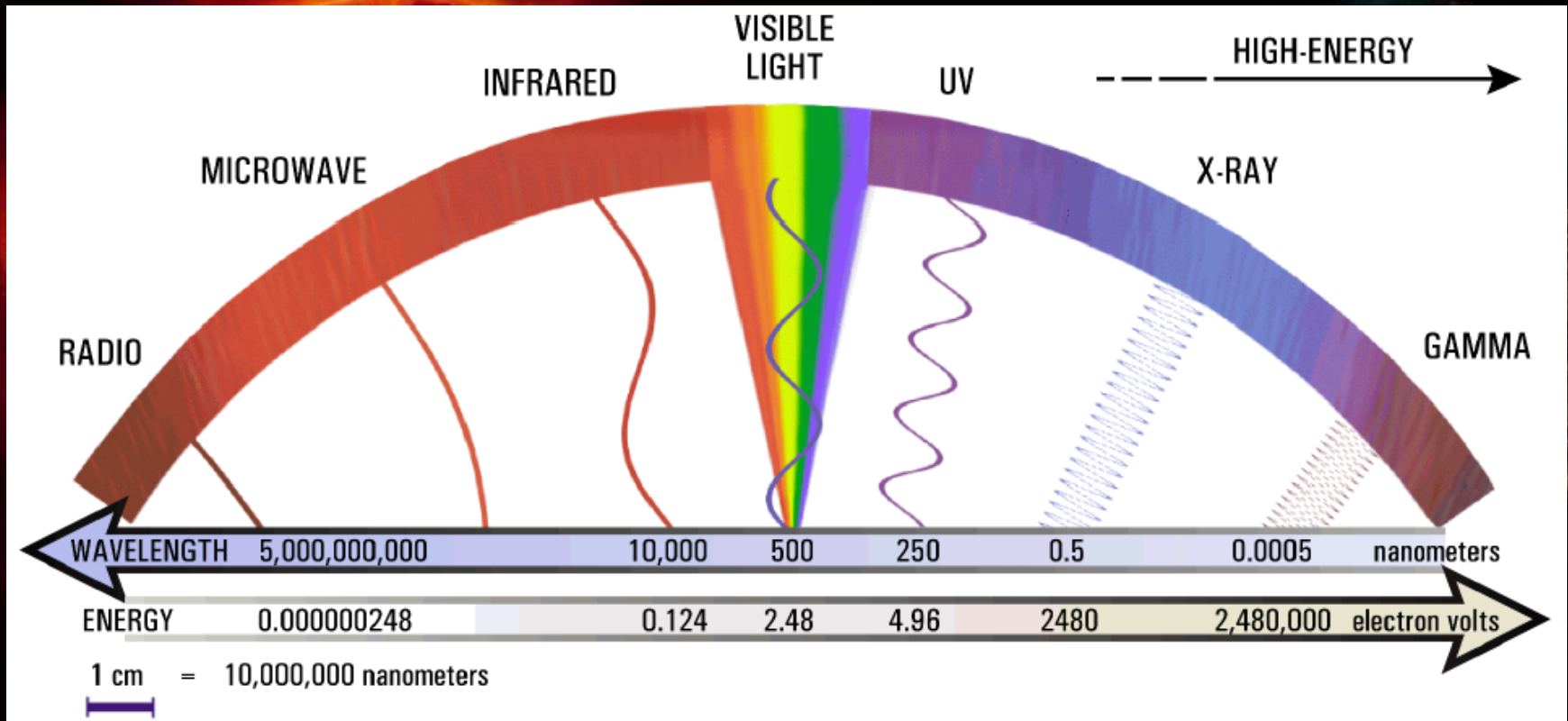


NASA/CXC/SAO/MPE



nasa.gov

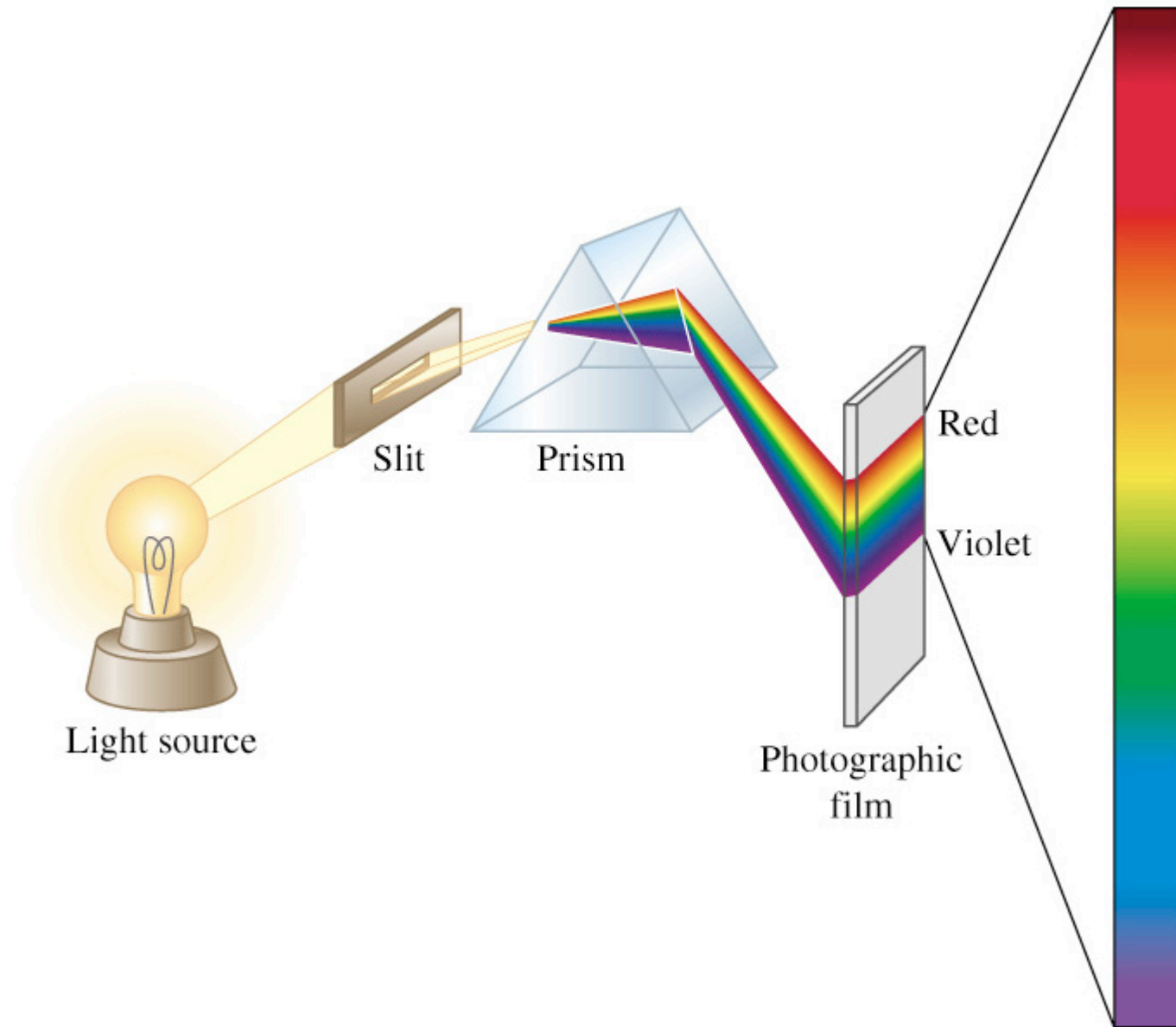
Photons in the universe



NASA/CXC/SAO/MPE

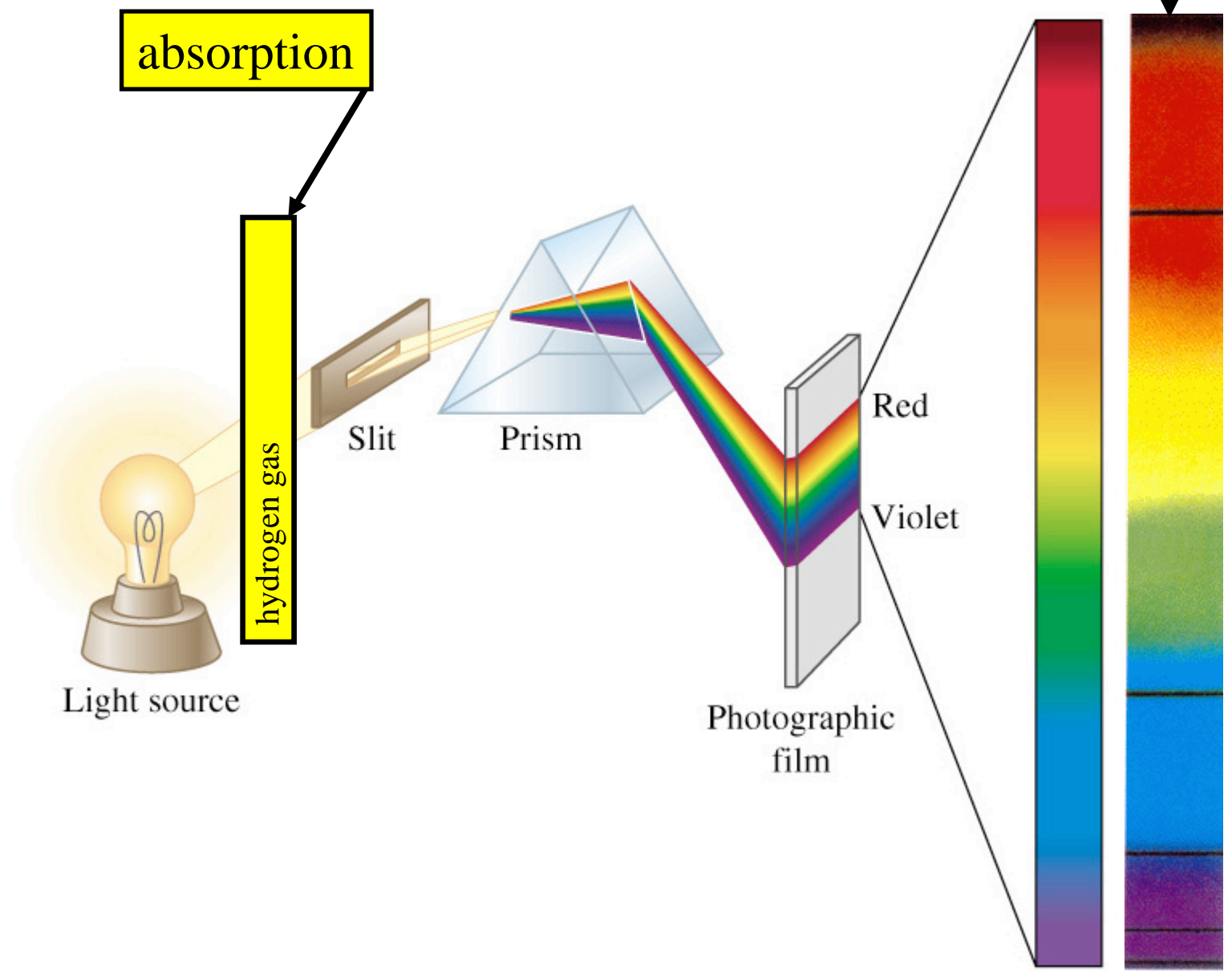
nasa.gov

Element production on the sun

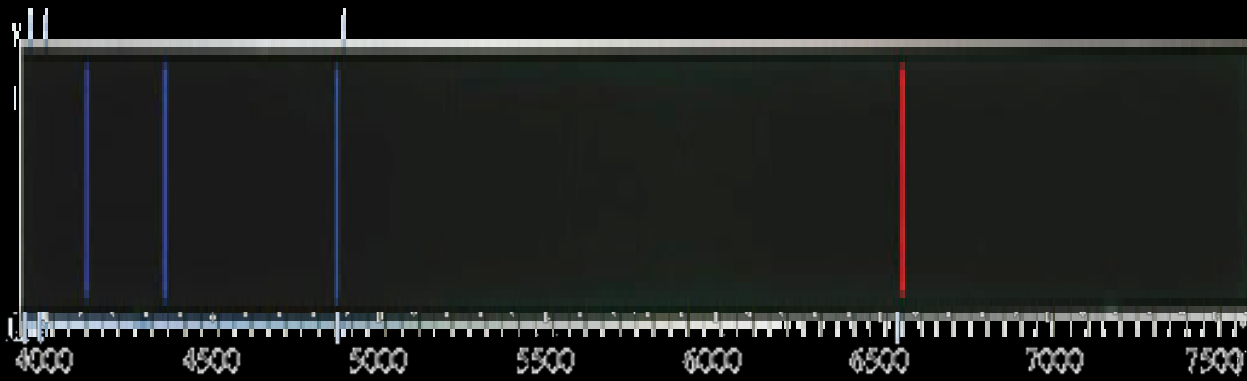


Spectral lines of hydrogen

absorption spectrum



Hydrogen emission spectrum



wave length nm



Spectral analysis

H



H δ

H γ

H β

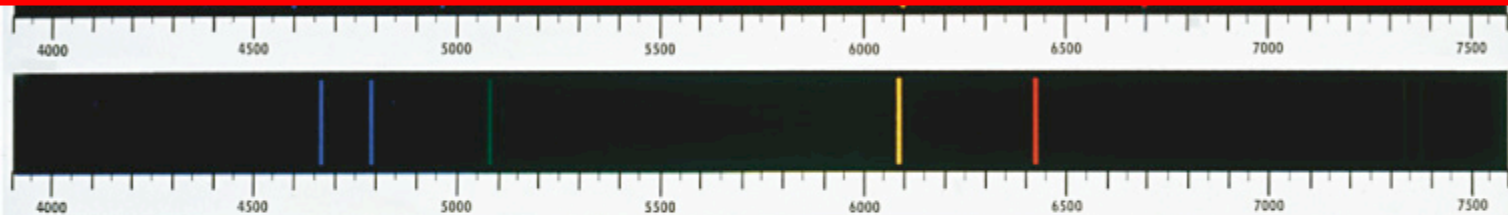
H α

Spectral analysis

Kirchhoff und Bunsen:

Every element has a characteristic emission band

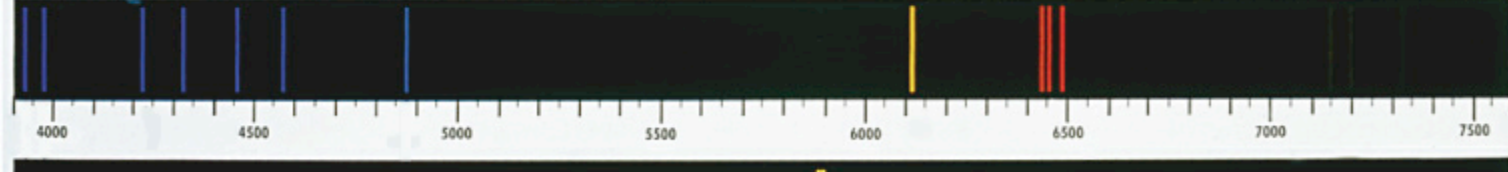
Cd



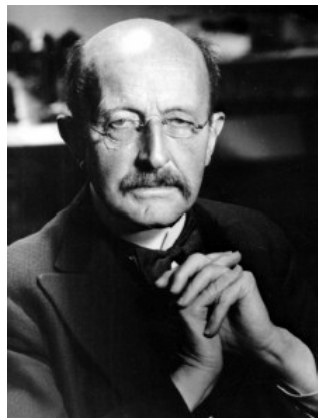
Sr



Ca

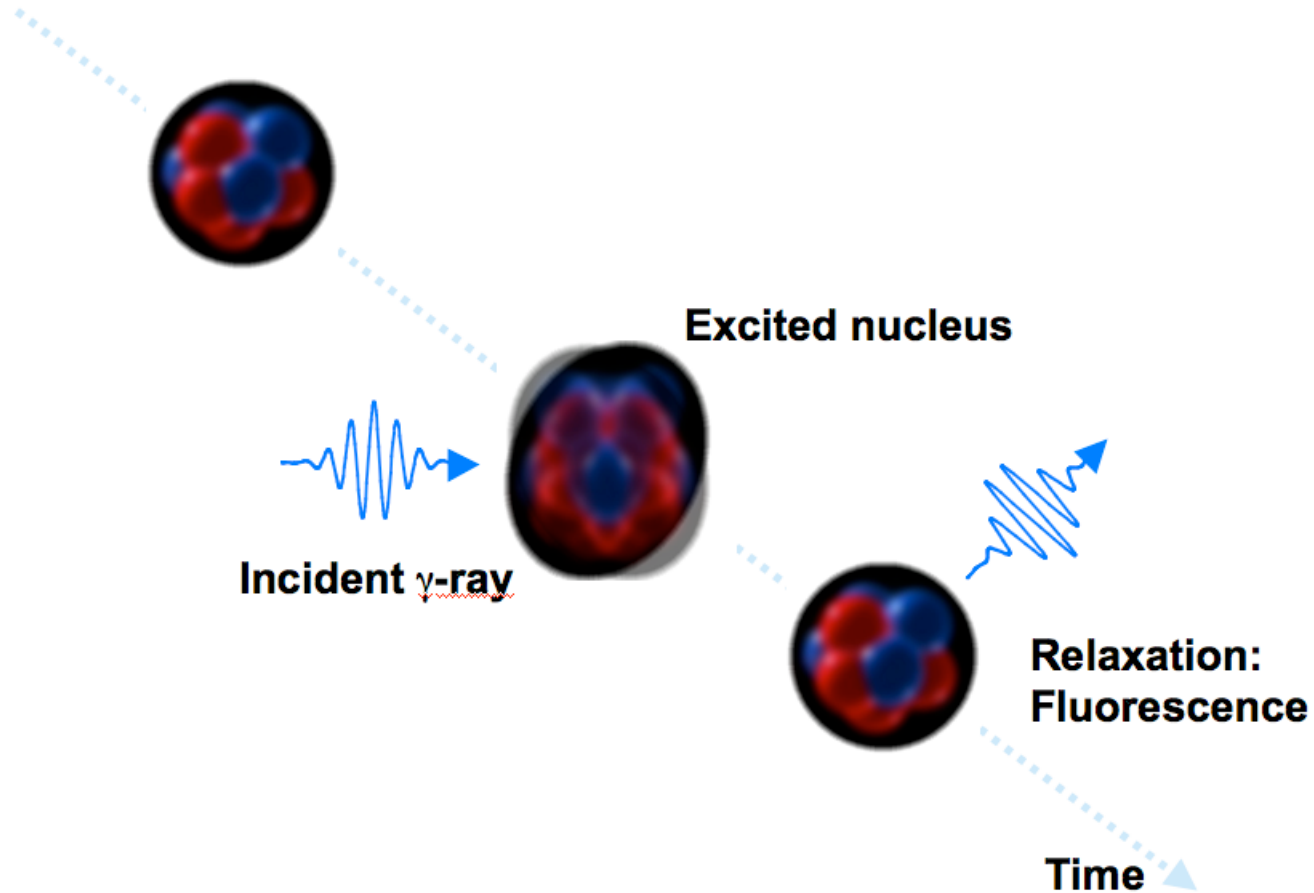


Na



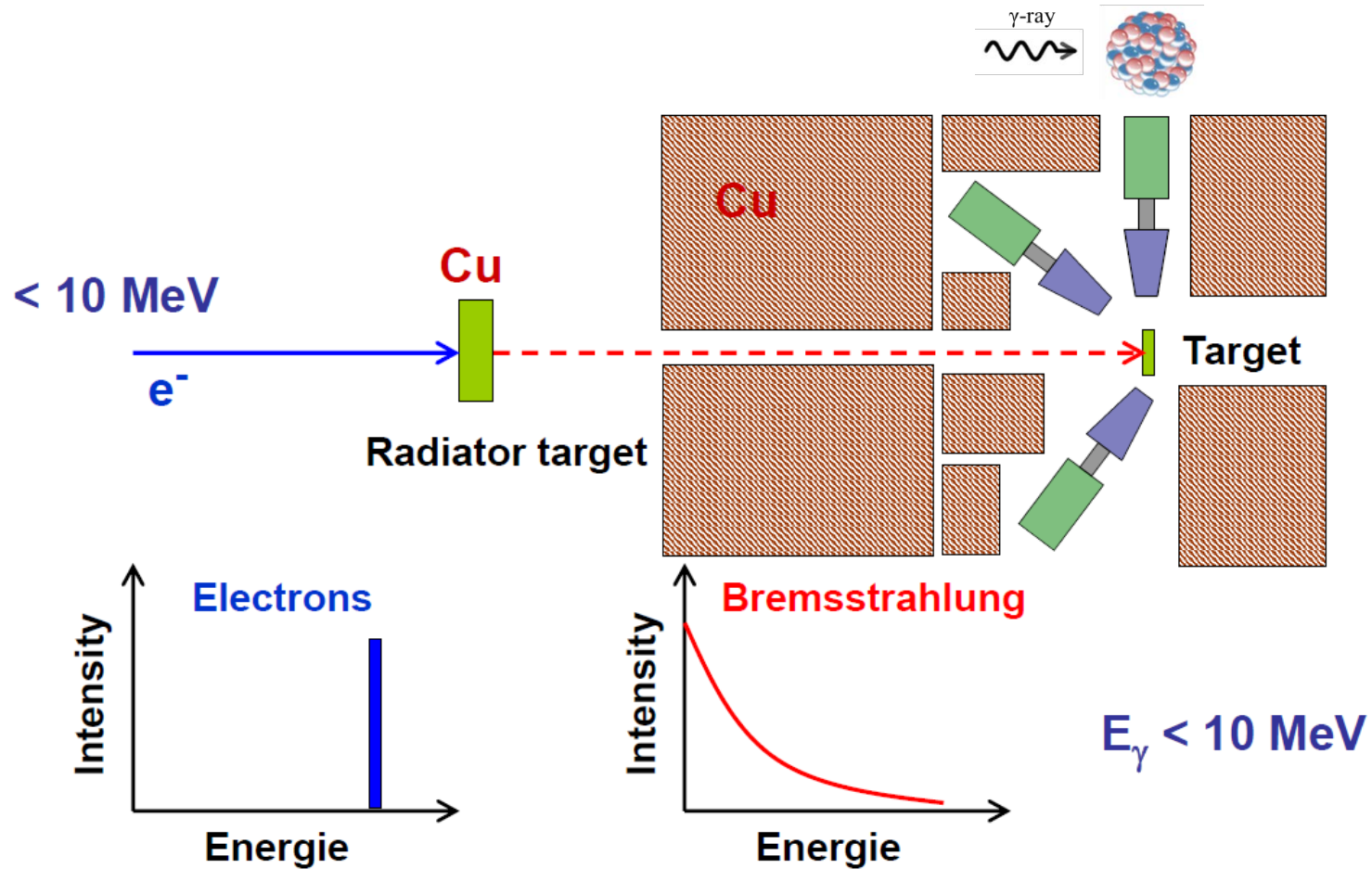
Max Planck

Nuclear Resonance Fluorescence



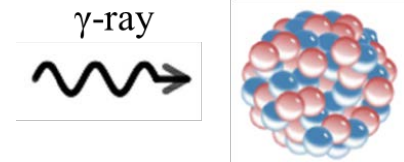
Nuclear Resonance Fluorescence (NRF) is analogous to atomic resonance fluorescence but depends upon the number of protons AND the number of neutrons in the nucleus

Low energy photon scattering at S-DALINAC

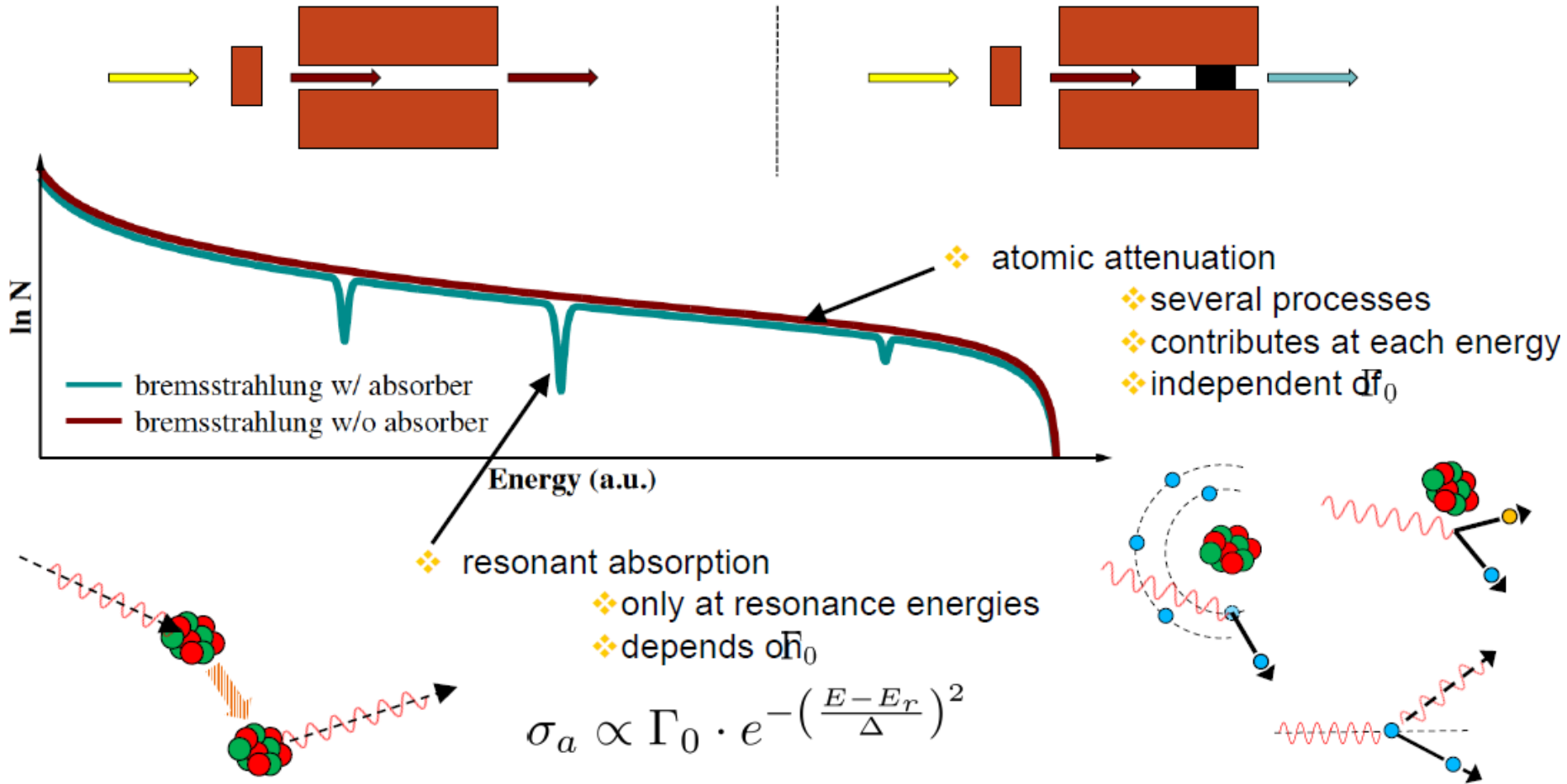


- “white“ photon spectrum
- wide energy region examined

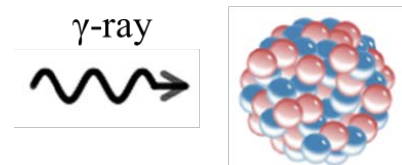
Absorption processes



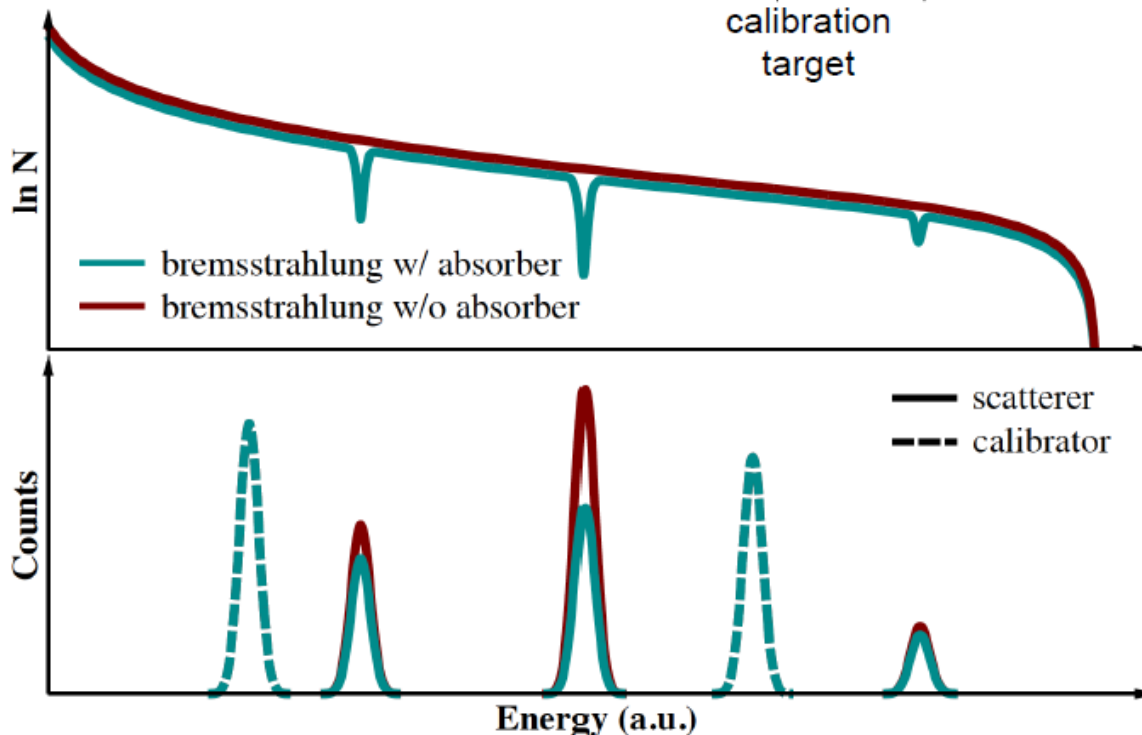
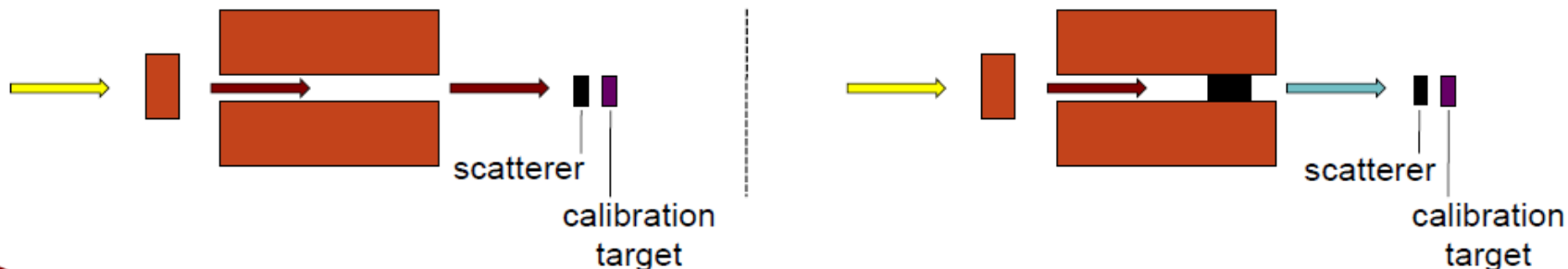
Absorption lines only a few eV wide!



Principle of measurement and self absorption



Use scatterer made of absorber material as „high-resolution detector“.

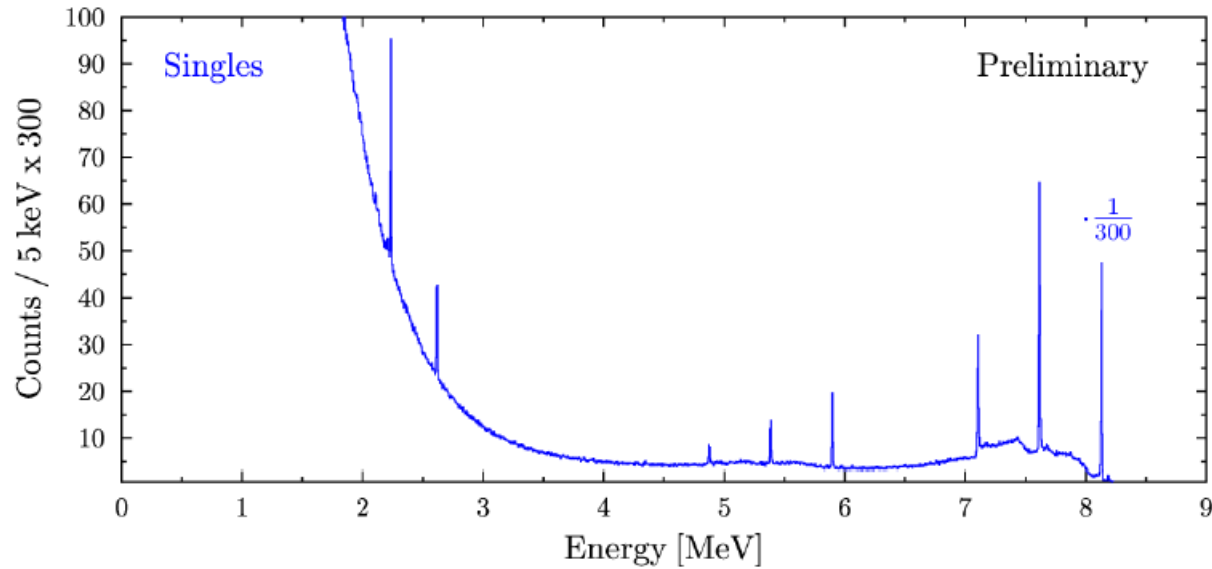


Self Absorption:
Decrease of Scattered Photons
because of Resonant Absorption

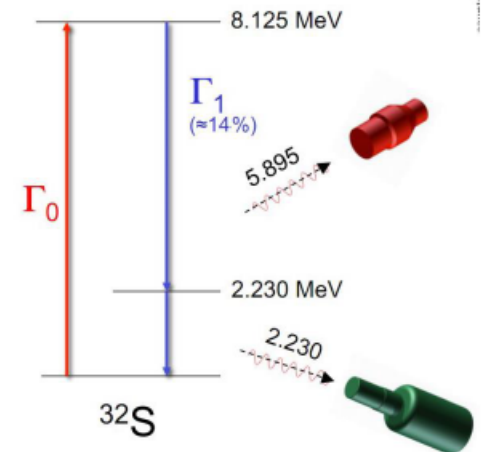
$$R(\Gamma_0) = \frac{N_{\text{woA}} - f \cdot N_{\text{wA}}}{N_{\text{woA}}}$$

$$f = \frac{N_{\text{woA}}^{\text{std}}}{N_{\text{wA}}^{\text{std}}}$$

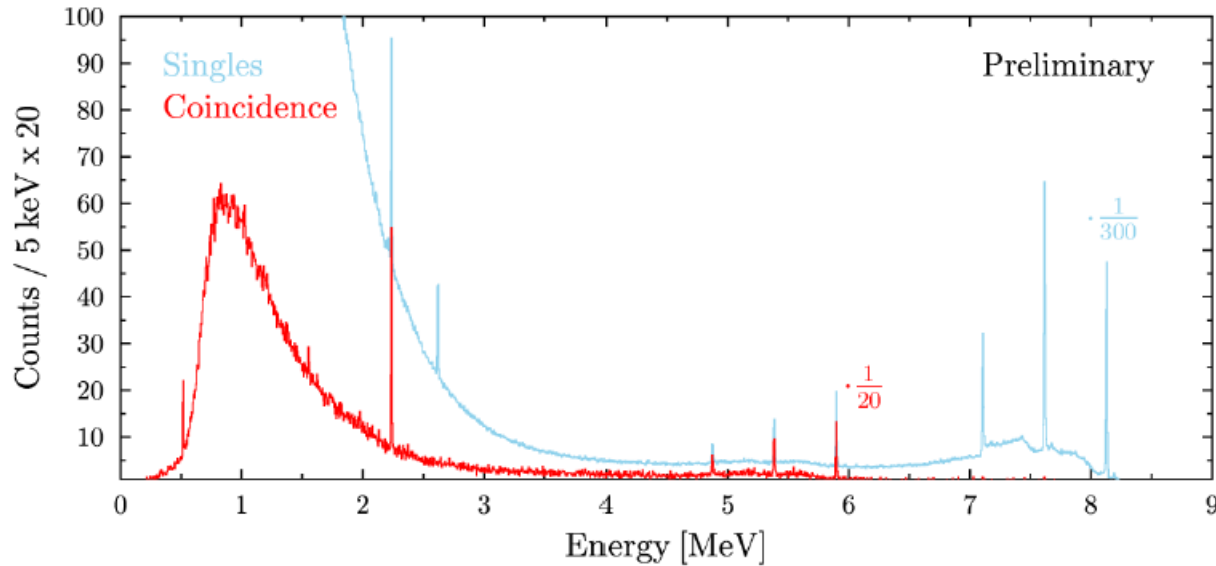
First γ -coincidences in a γ -beam



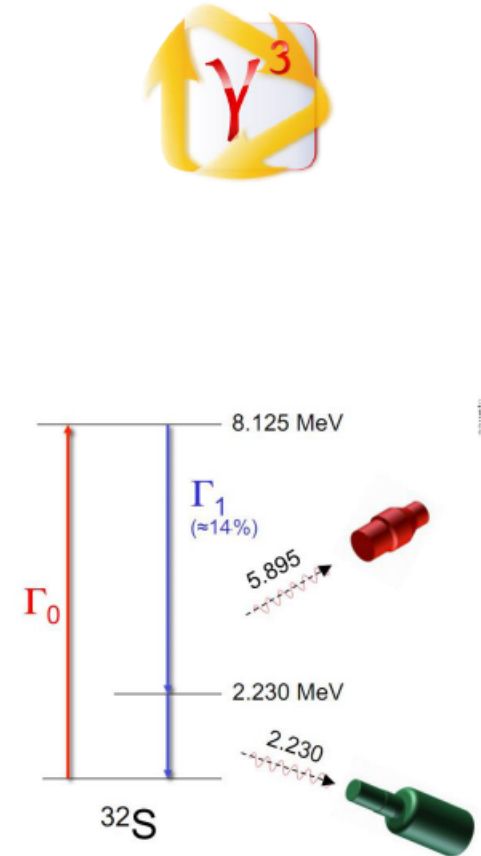
B. Löher et al., Nucl. Instruments Methods Phys. Res. Sect. A **723**, 136–142 (2013).



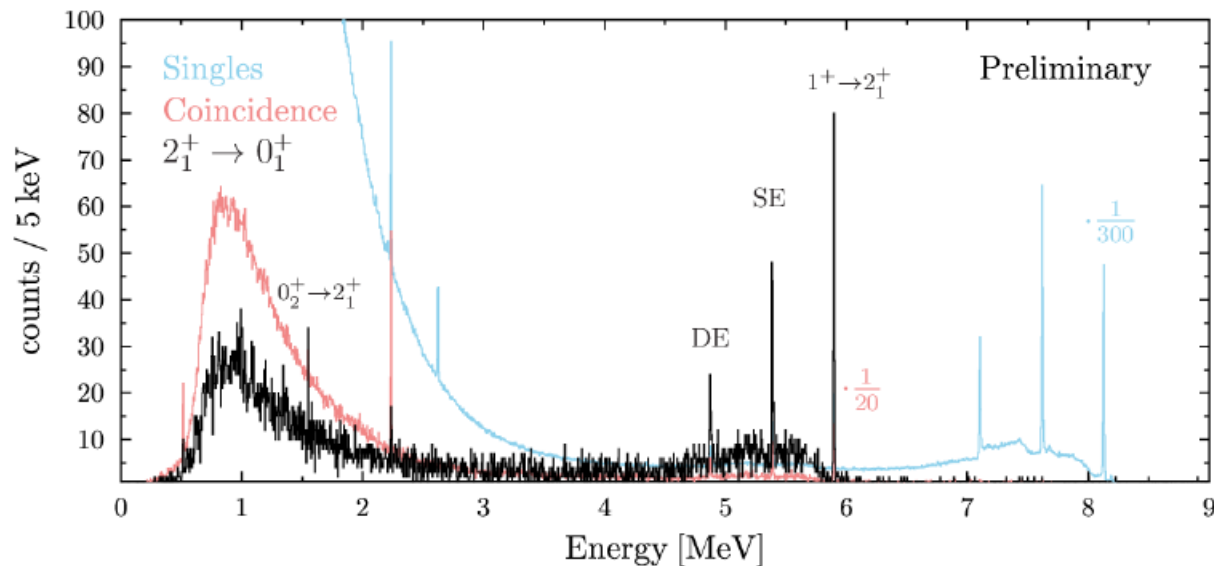
First γ -coincidences in a γ -beam



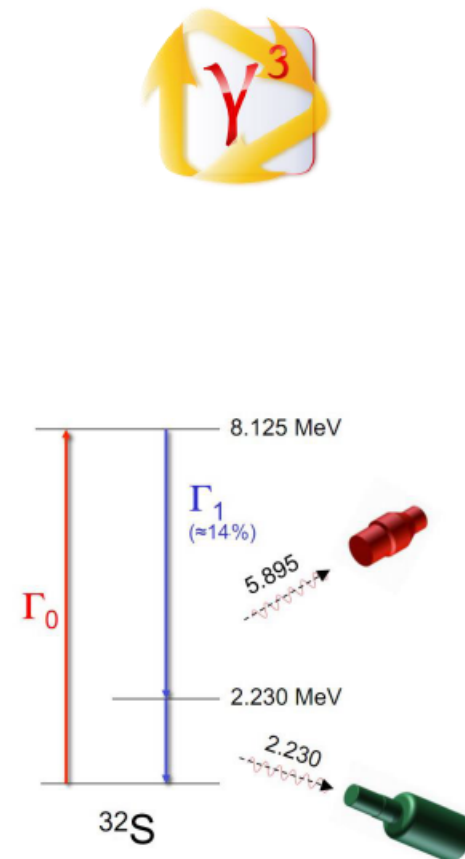
B. Löher et al., Nucl. Instruments Methods Phys. Res. Sect. A **723**, 136–142 (2013).



First γ -coincidences in a γ -beam



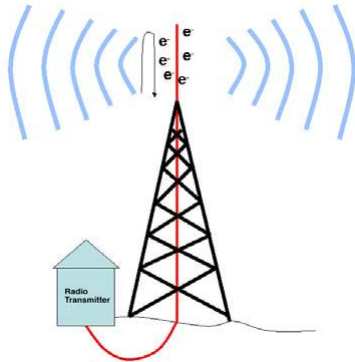
B. Löher et al., Nucl. Instruments Methods Phys. Res. Sect. A **723**, 136–142 (2013).





What is synchrotron radiation?

Electromagnetic radiation is emitted by charged particles when accelerated



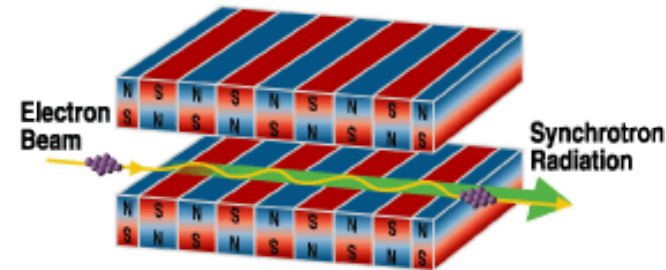
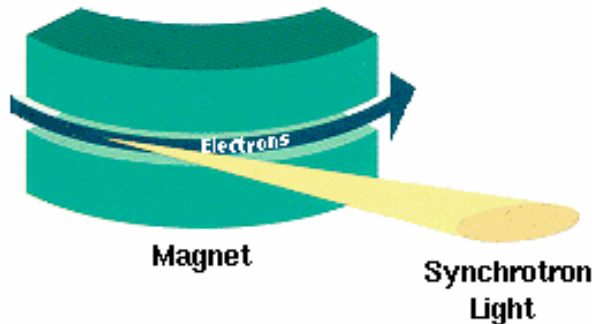
EM radiated from an antenna:
time-varying current runs up and down the
antenna, and in the process emits radio waves



At the heart of the Crab nebula is a rapidly-spinning
neutron star, a pulsar, and it powers the strongly
polarized bluish 'synchrotron' nebula.

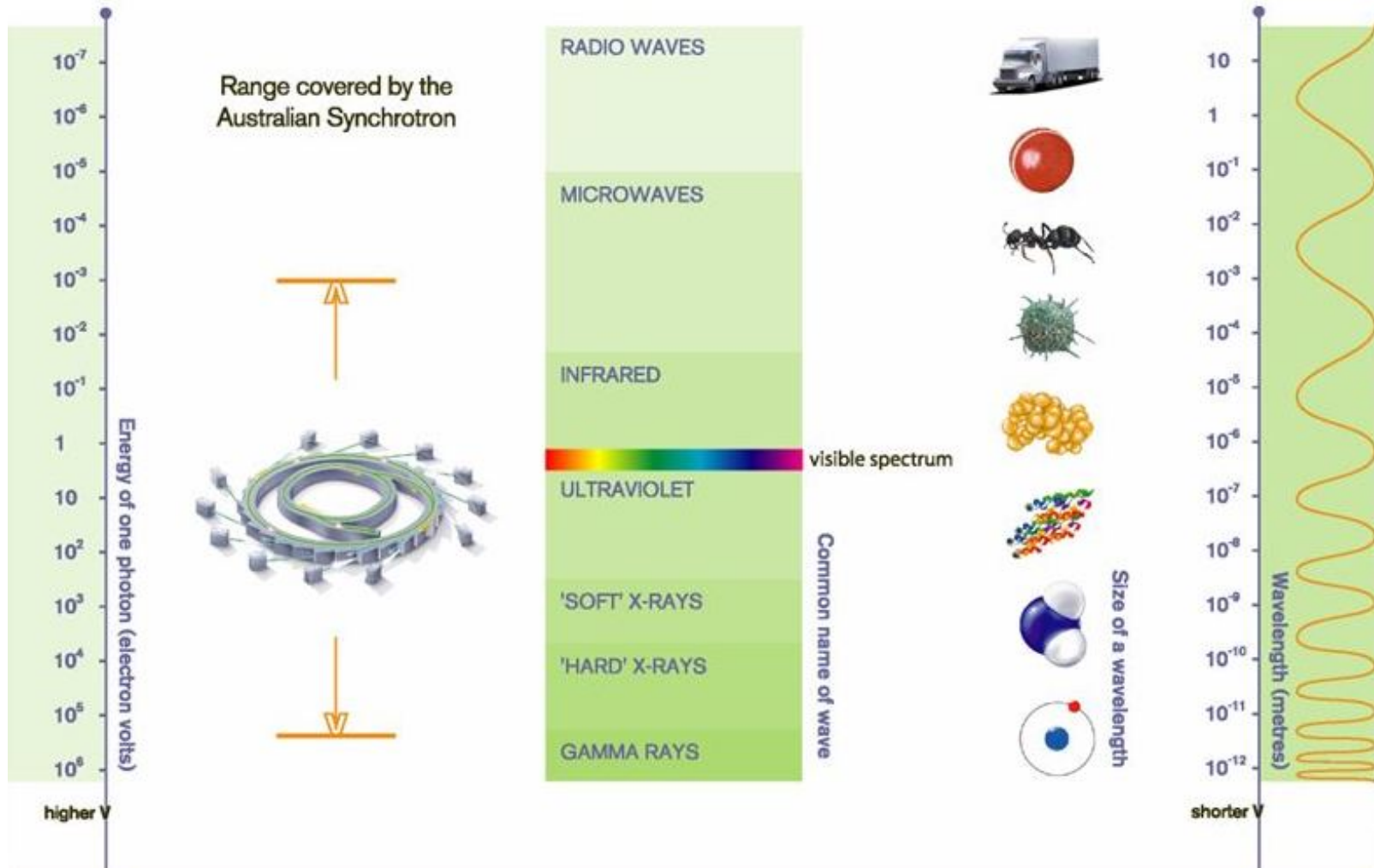
The electromagnetic radiation emitted when the charged particles are accelerated radially ($v \perp a$) is called **synchrotron radiation**.

It is produced in the synchrotron radiation source using bending magnets, undulators and wigglers



Properties of Synchrotron Radiation: Radiation Spectrum

The Electromagnetic Spectrum



Discovery of X-rays ~100 years ago



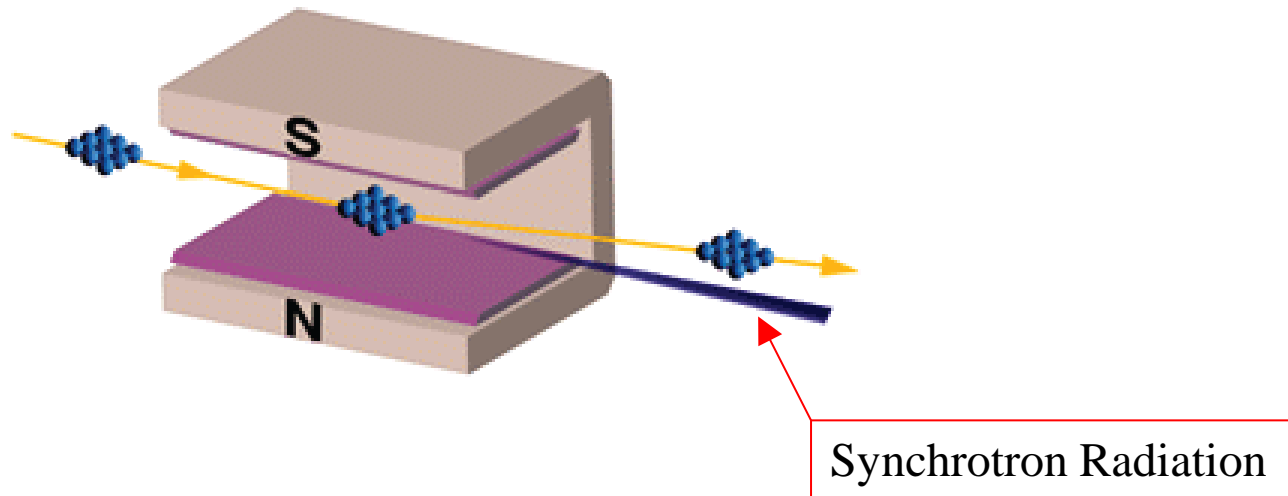
- ❖ X-rays were discovered (accidentally) in 1895 by Wilhelm Konrad Roentgen.
- ❖ Roentgen won the first Nobel Prize in 1901 “for the discovery with which his name is linked for all time: the ... so-called Roentgen rays, as he himself called them, X-rays ...”



first commercial X-ray tube

Synchrotron Radiation

Lorentz Force: $\vec{F} = q \cdot (\vec{E} + \vec{v} \times \vec{B})$

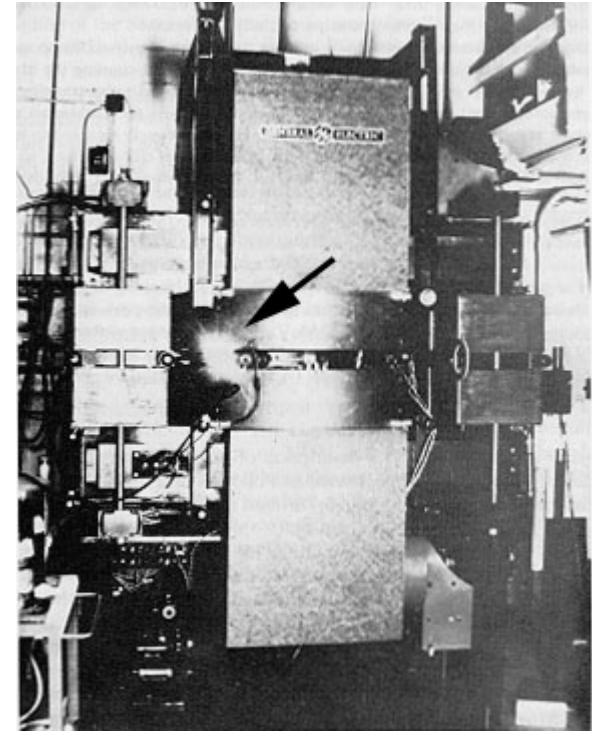


Electromagnetic radiation produced by relativistic charged particles accelerated in circular orbits.

Discovery of Synchrotron Radiation ~50 years ago

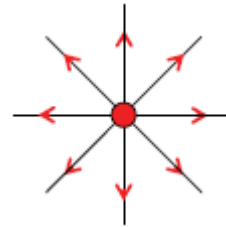
Synchrotron radiation was first observed (accidentally) from a 70 MeV synchrotron in 1947

On April 24, 1947 Langmuir and I [Herbert Pollack] were running the machine and as usual were trying to push the electron gun and its associated pulse transformer to the limit. Some intermittent sparking had occurred and we asked the technician to observe with a mirror around the protective concrete wall. He immediately signaled to turn off the synchrotron as “he saw an arc in the tube”. The vacuum was still excellent, so Langmuir and I came to the end of the wall and observed. At first we thought it might be due to Cherenkov radiation, but it soon became clear that we were seeing Ivanenko and Pomeranchuk [i.e. synchrotron] radiation.

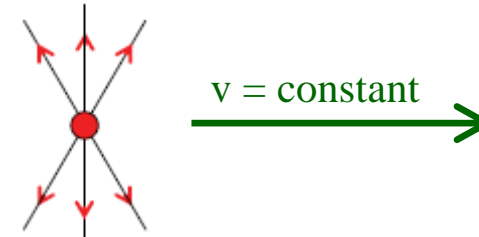


Radiation from moving charges

Charge at rest: Coulomb field, no radiation

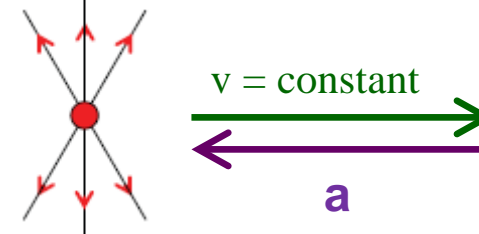


Uniformly moving charge, no radiation
(Cherenkov radiation)

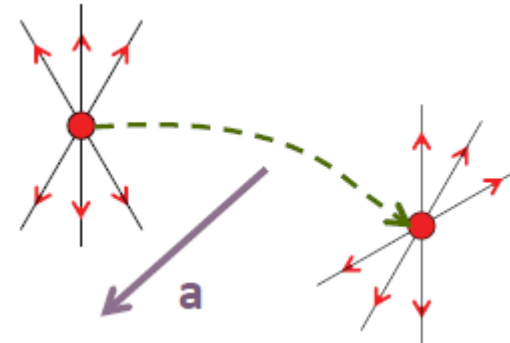


Accelerating charge

➤ $v \parallel a \rightarrow$ *Bremsstrahlung*, antennas

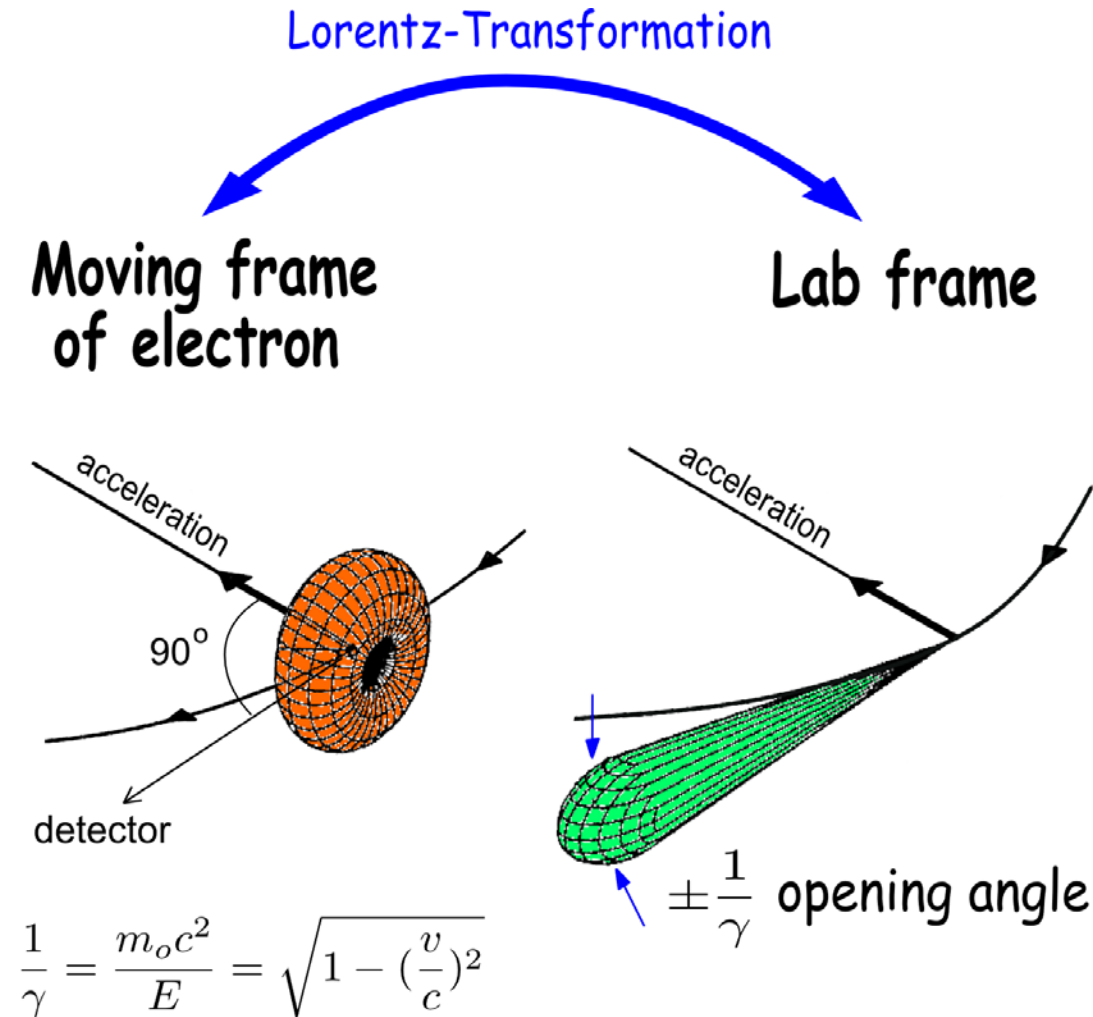


➤ $v \perp a \rightarrow$ *Synchrotron radiation*



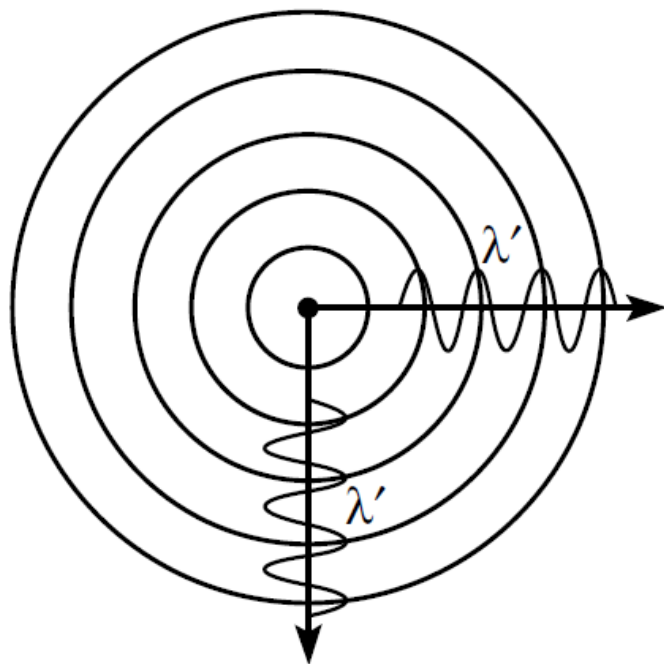
Properties of Synchrotron Radiation: Angular Distribution

- ❖ Radiation becomes more focused at higher energies



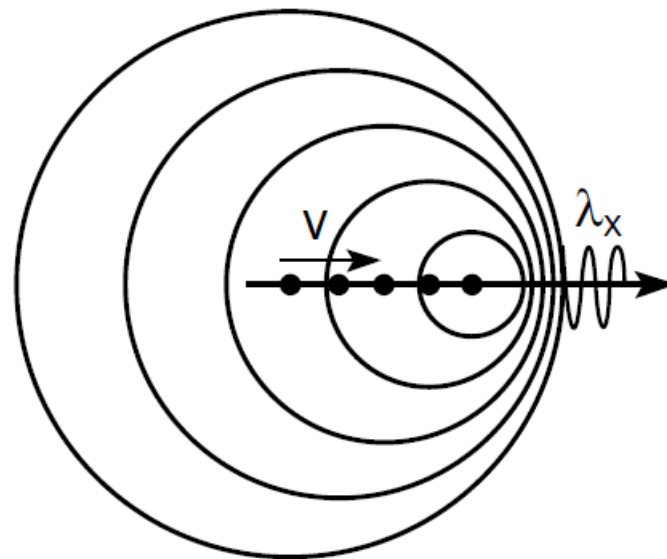
Synchrotron radiation from relativistic electrons

$v \ll c$



$$\lambda \cong \lambda' \cdot (1 - \beta \cdot \cos\theta)$$

$v \lesssim c$

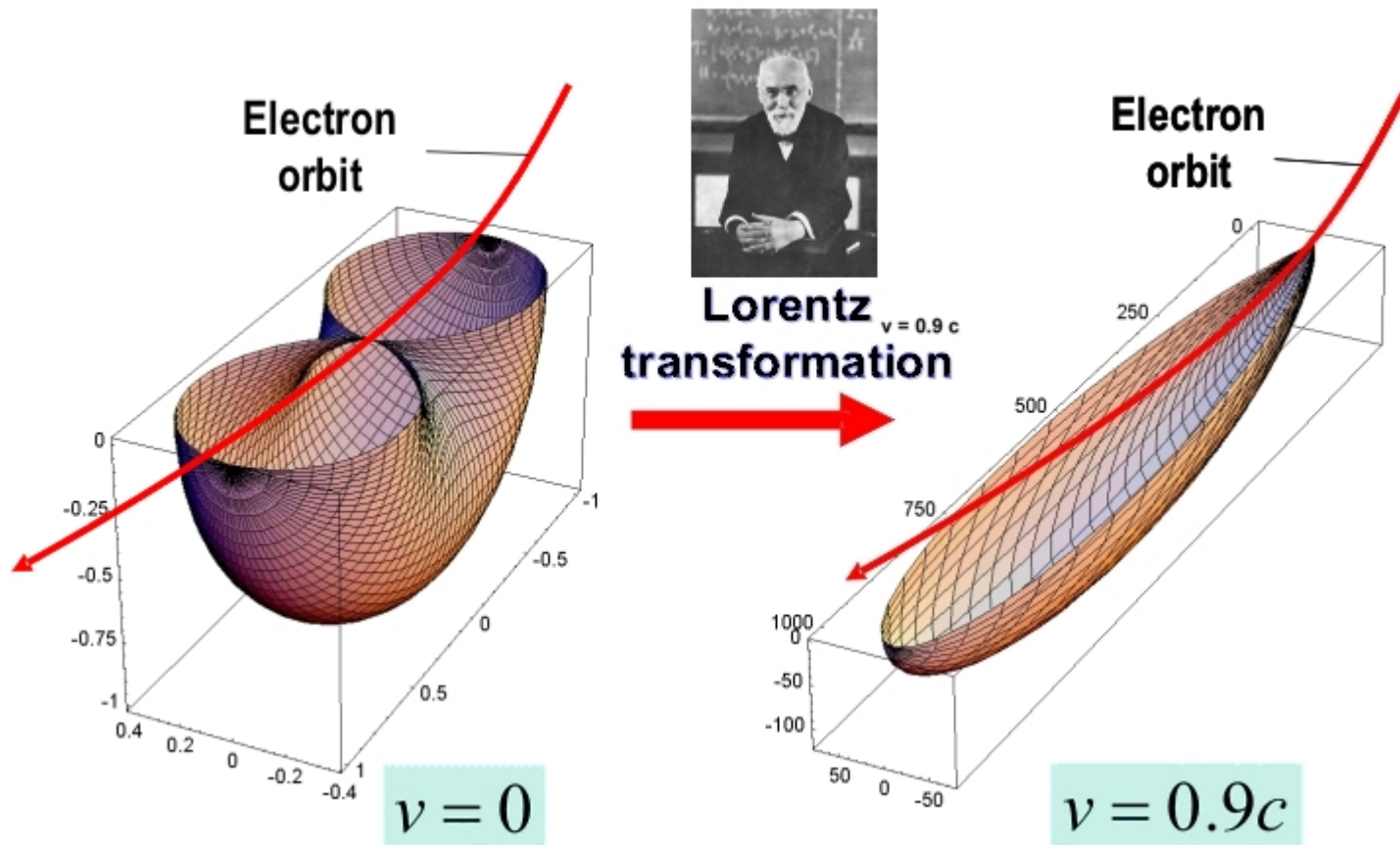


angle dependent Doppler shift

$$\lambda = \lambda' \cdot \frac{1 - \beta \cdot \cos\theta}{\sqrt{1 - \beta^2}}$$

$$E_\gamma = E_{\gamma 0} \cdot \frac{\sqrt{1 - \beta^2}}{1 - \beta \cdot \cos\theta}$$

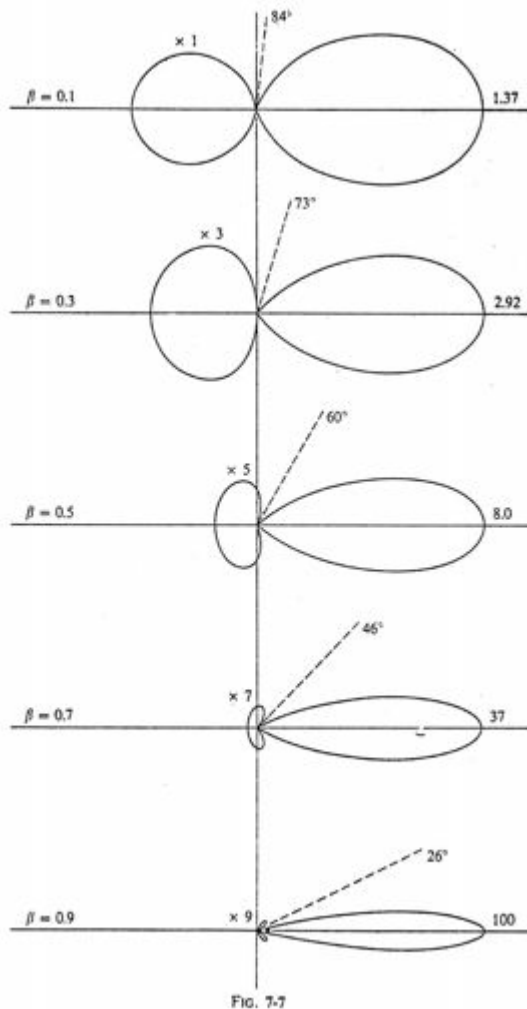
Synchrotron radiation from relativistic electrons



$$\frac{d\Omega_{rest}}{d\Omega_{lab}} = \left(\frac{E_\gamma}{E_{\gamma 0}} \right)^2$$

$$\frac{E_\gamma}{E_{\gamma 0}} = \frac{\sqrt{1 - \beta^2}}{1 - \beta \cdot \cos\theta}$$

Radiation Patterns when ν approaches c



As β approaches 1:

- The shape of the radiation pattern is changing; it is more forward peaked
- The size of the radiation pattern is changing; it is getting bigger

So at $\beta \approx 1$, the node at $\theta' = 90^\circ$ (in the frame of the radiating particle, rest frame) transforms to:

$$\tan\theta_{lab} = \frac{\sin\theta'}{\gamma \cdot (\cos\theta' + \beta)} = \frac{1}{\gamma \cdot \beta} \approx \frac{1}{\gamma}$$

In fact, the *opening angle* in both the horizontal and vertical directions, is given approximately by:

$$\theta = \frac{1}{\gamma}$$

Synchrotron Radiation

Consider a charged particle in homogeneous field B

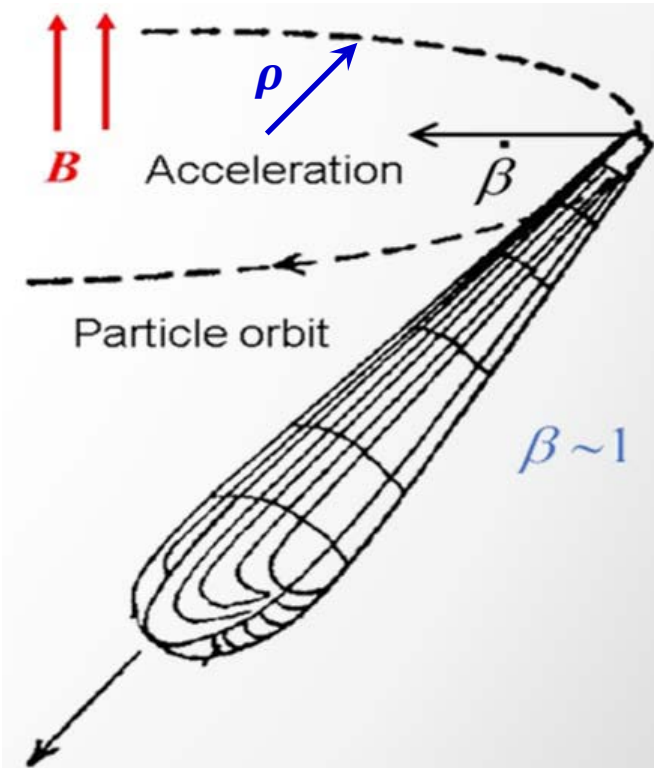
❖ The acceleration in B is given by

$$\dot{\vec{\beta}}_{\perp} = \frac{\beta^2 c}{\rho} \quad m\dot{v} = \frac{mv^2}{\rho}$$

where the bending radius of charged particle, ρ , at energy E_e is

$$\frac{1}{\rho[m]} = \frac{e \cdot B \cdot c}{\beta \cdot E_e} = 0.2998 \frac{B[T]}{\beta \cdot E_e[GeV]}$$

Larmor radius $\rho = \frac{mv}{e \cdot B} = \frac{mc^2 \cdot v}{e \cdot B \cdot c^2} = \frac{E_e \cdot \beta}{e \cdot \beta \cdot c}$



Then the instantaneous radiation power becomes

$$P = \frac{2 \cdot c \cdot r_e \cdot m_e c^2}{3} \cdot \frac{\beta^4 \cdot \gamma^4}{\rho^2} = \frac{c \cdot C_{\gamma}}{2\pi} \cdot \frac{E_e^4}{\rho^2}$$

$$C_{\gamma} \equiv \frac{4\pi}{3} \cdot \frac{r_e}{(m_e c^2)^3} = 8.85 \cdot 10^{-5} \left[\frac{m}{GeV^3} \right]$$

classical electron radius $r_e = \frac{e}{4\pi \cdot \epsilon_0 \cdot m_e c^2}$

Synchrotron Radiation Power and Energy Loss for Electrons

- ❖ Instantaneous Synchrotron Radiation Power for a single **electron**

$$P_\gamma [\text{GeV}/\text{s}] = \frac{c \cdot C_\gamma}{2\pi} \cdot \frac{E^4 [\text{GeV}^4]}{\rho^2 [\text{m}^2]} \quad \text{with} \quad C_\gamma = 8.8575 \cdot 10^{-5} \frac{m}{\text{GeV}^3}$$

- ❖ Energy loss per turn for a single particle in an isomagnetic lattice with bending radius ρ is given by integrating P_γ over the lattice

$$\Delta E [\text{GeV}] = C_\gamma \cdot \frac{E^4 [\text{GeV}^4]}{\rho [\text{m}]}$$

- ❖ The average Radiated Power for an entire beam is ($P = I/e \cdot \Delta E$)

$$P_\gamma [\text{MW}] = 8.8575 \cdot 10^{-2} \cdot \frac{E^4 [\text{GeV}^4]}{\rho [\text{m}]} \cdot I [\text{A}]$$

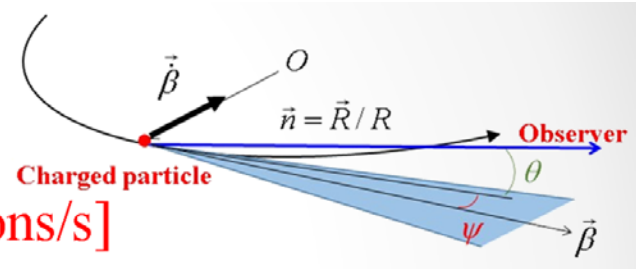
- ❖ Radiated Power varies as the **inverse fourth power of particle mass**. Comparing radiated power from a proton vs. an electron, we have: $\frac{P_e}{P_p} = \left(\frac{m_p}{m_e}\right)^4 = 1836^4 = 1.1367 \cdot 10^{13}$

$$P_\gamma [\text{MW}] = 2.65 \cdot 10^{-2} \cdot E^3 [\text{GeV}]^3 \cdot B [\text{T}] \cdot I [\text{A}]$$

Synchrotron Radiation Photon Numbers

❖ Total photon numbers

$$\begin{aligned}\dot{N}_{ph, Ie} &= \frac{15\sqrt{3}\pi}{4} C_{\psi} I_e E_e \\ &= 8.08 \times 10^{20} I[A] E_e[\text{GeV}] \quad [\text{photons/s}]\end{aligned}$$



Some useful formulas for synchrotron radiation

$$\gamma = \frac{1}{\sqrt{1 - \frac{v^2}{c^2}}} = \frac{1}{\sqrt{1 - \beta^2}}; \quad \beta = \frac{v}{c}; \quad (1 - \beta) \cong \frac{1}{2\gamma^2}$$

$$E_e = \gamma \cdot mc^2; \quad p = \gamma \cdot mv$$

$$\gamma = \frac{E_e}{mc^2} = 1957 \cdot E_e [\text{GeV}]$$

$$\hbar\omega \cdot \lambda = 1239.842 [\text{eV} \cdot \text{nm}]$$

$$1 \text{ Watt} \Rightarrow 5.034 \cdot 10^{15} \cdot \lambda [\text{nm}] \cdot \frac{\text{photons}}{\text{s}}$$

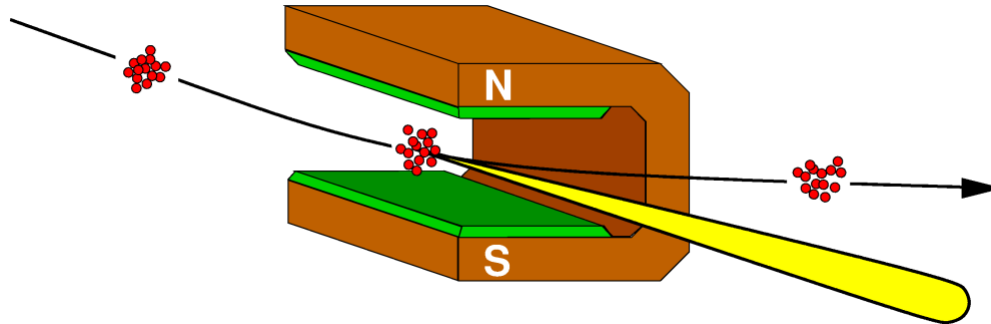
$$\text{Bending Magnet: } E_c = \frac{3e \cdot \hbar \cdot B \cdot \gamma^2}{2m}; \quad E_c(\text{keV}) = 0.6650 E_e^2 [\text{GeV}] \cdot B [\text{T}]$$

$$\text{Undulator: } \lambda = \frac{\lambda_u}{2\gamma^2} \cdot \left(1 + \frac{K^2}{2} + \gamma^2 \cdot \theta^2 \right); \quad E(\text{keV}) = \frac{0.9496 \cdot E_e^2 (\text{GeV})}{\lambda_u(\text{cm}) \cdot \left(1 + \frac{K^2}{2} + \gamma^2 \cdot \theta^2 \right)}$$

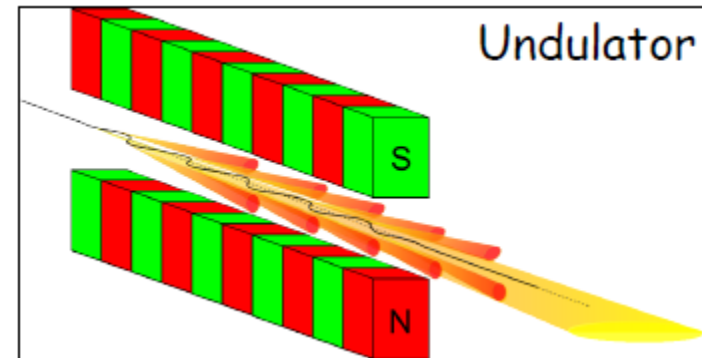
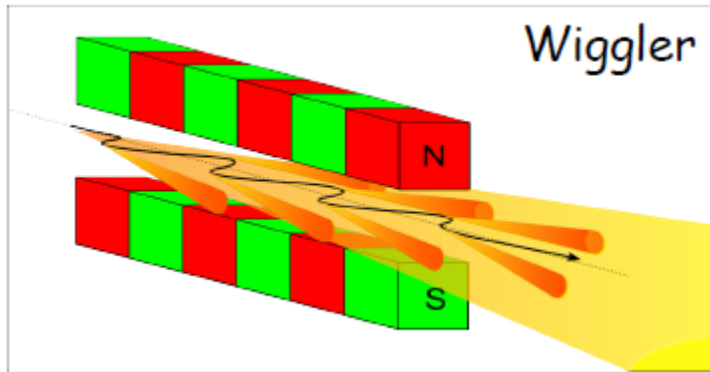
$$\text{where } K \equiv \frac{e \cdot B_0 \cdot \lambda_u}{2\pi \cdot mc} = 0.9337 \cdot B_0(\text{T}) \cdot \lambda_u(\text{cm})$$

Accelerator Synchrotron Sources

- ❖ Synchrotron radiation is generated in normal accelerator bending magnets



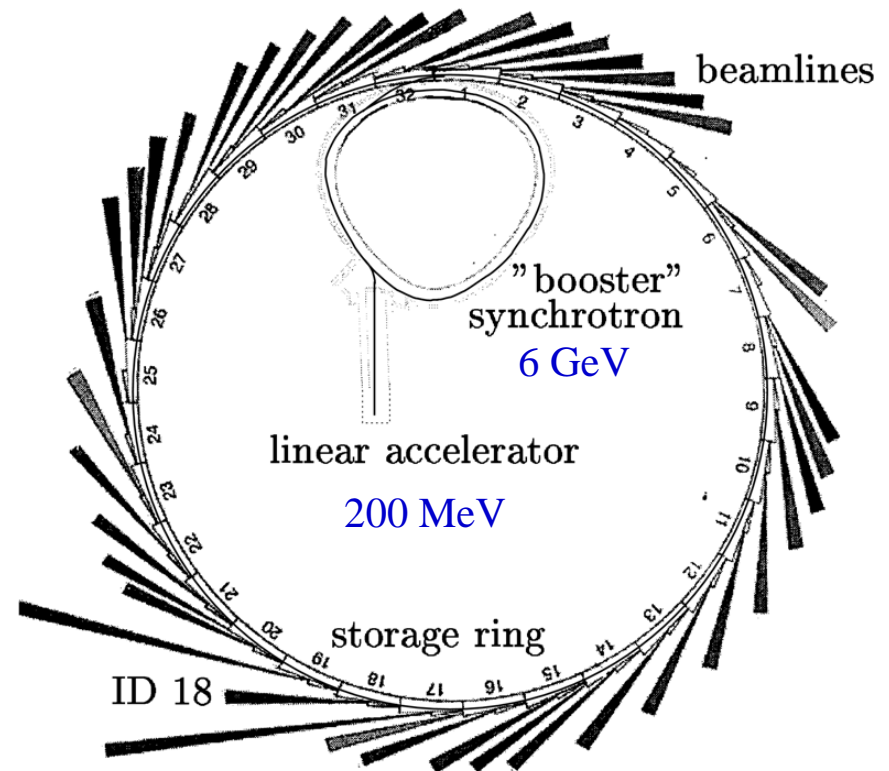
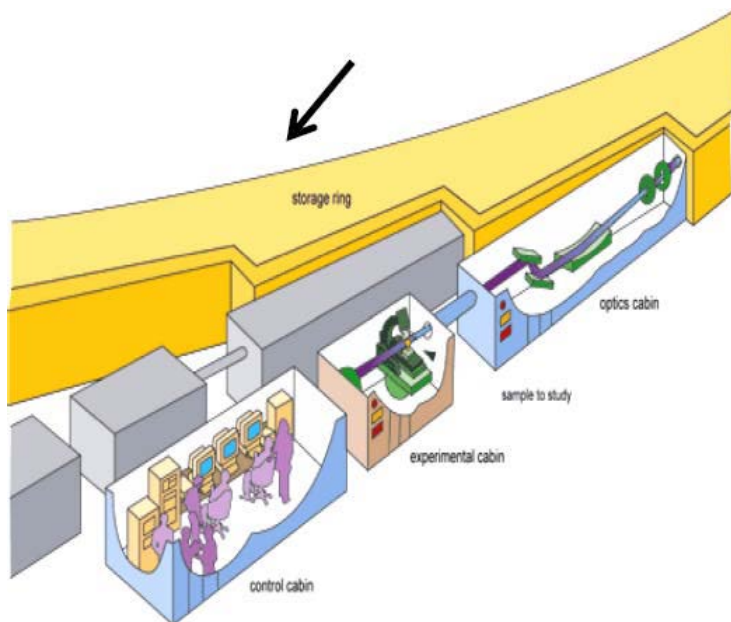
- ❖ There are also special magnets called wigglers and undulators which are designed for this purpose.



Layout of a synchrotron radiation source

Electrons are generated and accelerated in a *LINAC*, further accelerated to the required energy in a *booster* and injected and stored in a *storage ring*.

The circulating electrons emit an intense beam of synchrotron radiation which is sent down the beamlines.



Synchrotron Light Sources

Diamond



Indus-2



SOLEIL

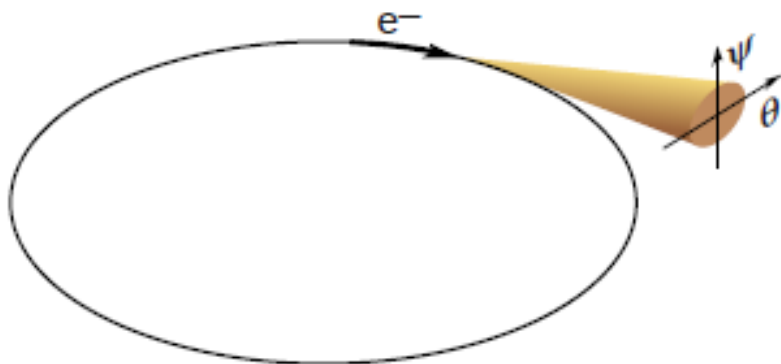


ASP



Synchrotron Radiation Spectrum

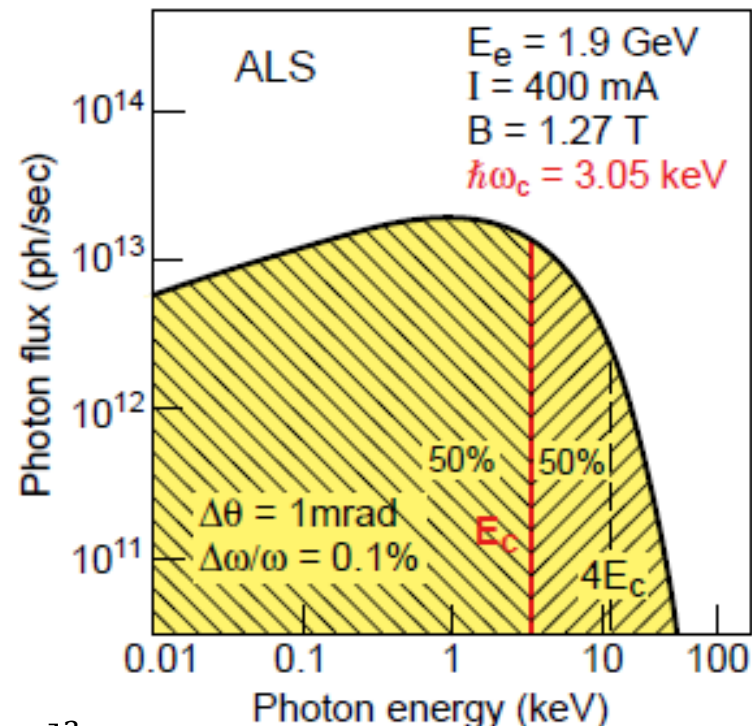
Bending Magnet Radiation covers a broad region of the spectrum, including the primary absorption edges of most elements.



$$E_c = \hbar\omega_c = \frac{3e \cdot \hbar \cdot B \cdot \gamma^2}{2m}$$

$$E_c(\text{keV}) = 0.6650 \cdot E_e^2(\text{GeV}) \cdot B(\text{T}) = 2.218 \cdot \frac{E_e^3[\text{GeV}]^3}{\rho[\text{m}]}$$

$$\frac{d^2 F_B}{d\theta d\omega/\omega} = 2.46 \cdot 10^{13} E_e(\text{GeV}) \cdot I(\text{A}) \cdot G_1(E/E_c) \cdot \frac{\text{photons/s}}{\text{mrad} \cdot (0.1\% \text{BW})}$$

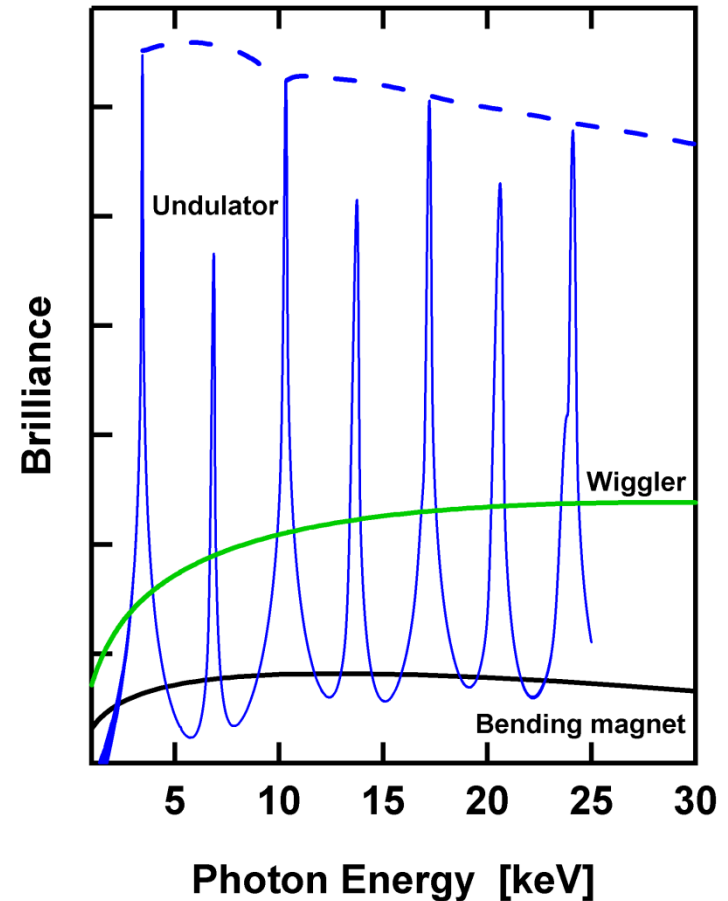


Advantages: cover broad spectral range
least expensive
most accessible

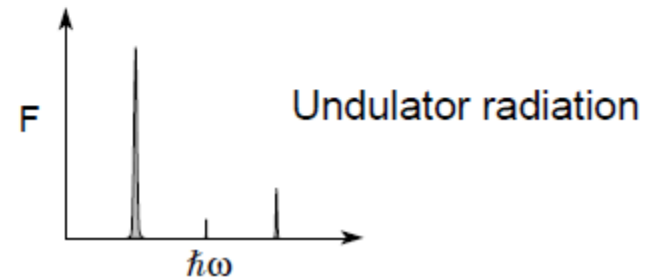
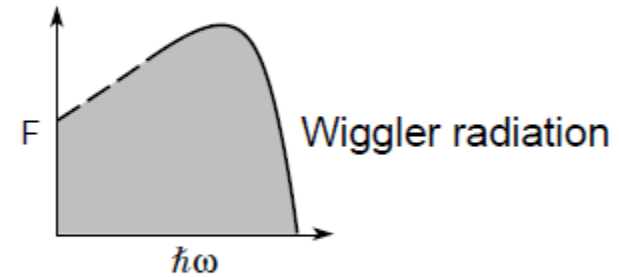
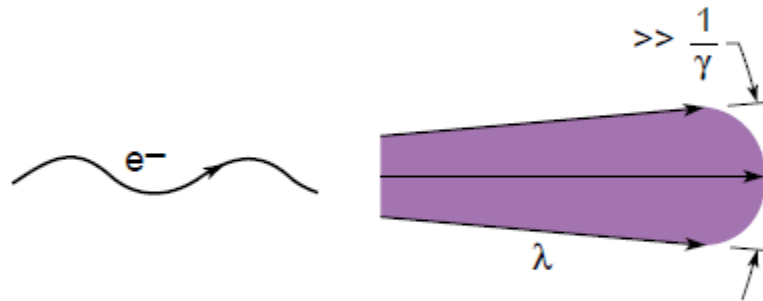
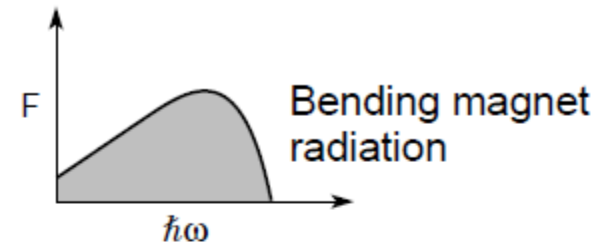
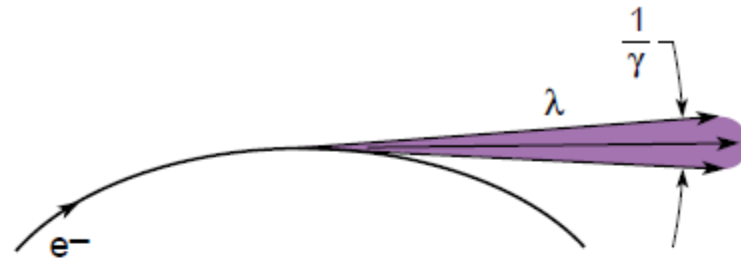
Disadvantages: limited coverage of hard X-rays
not as bright as undulator

Undulator: Electron beam is periodically deflected by a weak magnetic field. Particle emits radiation at wavelength of the periodic motion, divided by γ^2 . So period of cm for magnets results in radiation in VUV to X-ray regime.

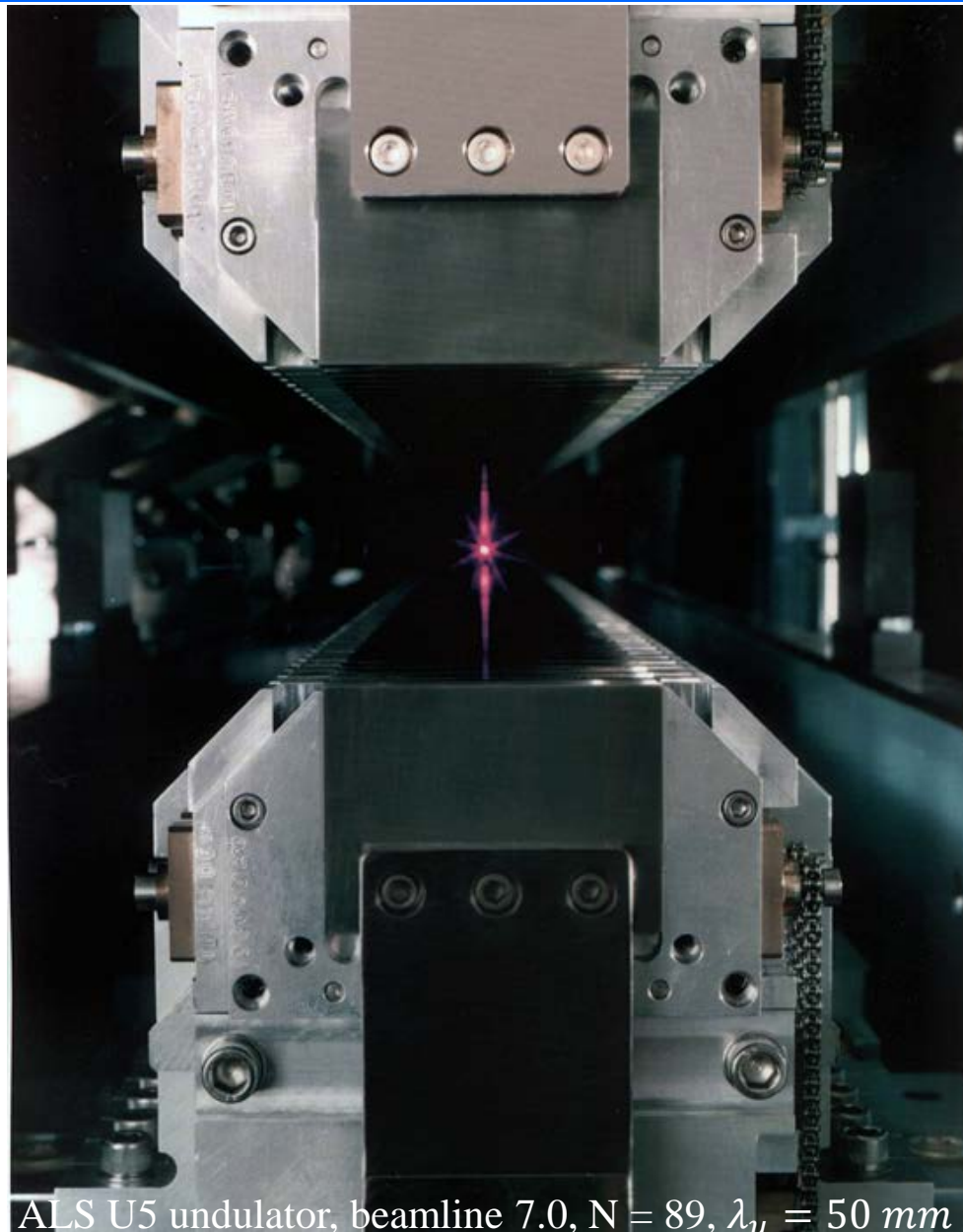
Wiggler: Electron beam is periodically deflected by strong bending magnets. Motion is no longer pure sinusoid and radiation spectrum is continuous up to a critical cut off photon energy ($\epsilon_{crit} \sim B \cdot \gamma^2$). Spectrum is infrared to hard X-rays.



Three Forms of Synchrotron Radiation



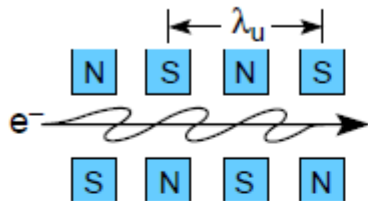
An Undulator up close



ALS U5 undulator, beamline 7.0, $N = 89$, $\lambda_u = 50 \text{ mm}$

Undulator Radiation

Laboratory Frame of Reference

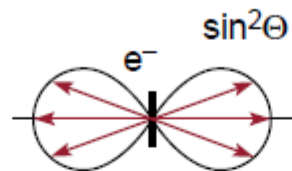


$$E = \gamma mc^2$$

$$\gamma = \frac{1}{\sqrt{1 - \frac{v^2}{c^2}}}$$

$N = \#$ periods

Frame of Moving e^-



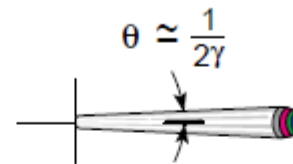
e^- radiates at the Lorentz contracted wavelength:

$$\lambda' = \frac{\lambda_u}{\gamma}$$

Bandwidth:

$$\frac{\lambda'}{\Delta\lambda'} \approx N$$

Frame of Observer



Doppler shortened wavelength on axis:

$$\lambda = \lambda' \gamma (1 - \beta \cos \theta)$$

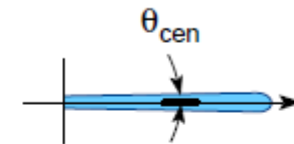
$$\lambda = \frac{\lambda_u}{2\gamma^2} (1 + \gamma^2 \theta^2)$$

Accounting for transverse motion due to the periodic magnetic field:

$$\lambda = \frac{\lambda_u}{2\gamma^2} \left(1 + \frac{K^2}{2} + \gamma^2 \theta^2 \right)$$

where $K = eB_0\lambda_u/2\pi mc$

Following Monochromator



$$\text{For } \frac{\Delta\lambda}{\lambda} \approx \frac{1}{N}$$

$$\theta_{\text{cen}} \approx \frac{1}{\gamma\sqrt{N}}$$

typically

$$\theta_{\text{cen}} \approx 40 \text{ rad}$$

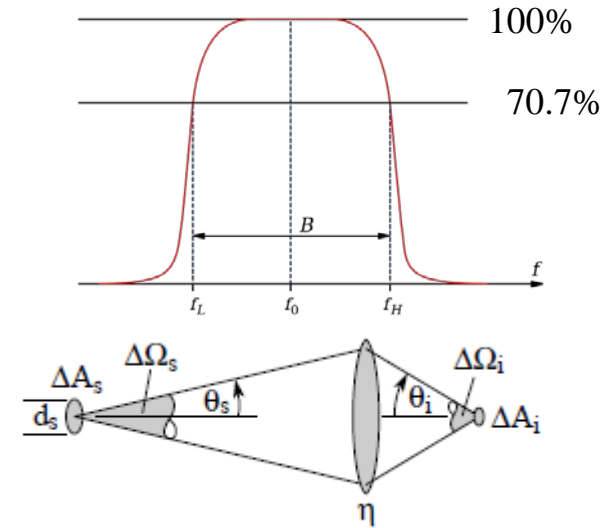
How to characterize the properties of a synchrotron radiation source?

$$\text{Total flux} \equiv \frac{\text{Photons}}{s}$$

$$\text{Spectral flux} \equiv \frac{\text{Photons}/s}{0.1\% \text{ bandwidth}}$$

$$\text{Brightness} \equiv \frac{\text{Photons}/s}{\text{mrad}^2 \cdot 0.1\% \text{ bandwidth}}$$

$$\text{Brilliance} \equiv \frac{\text{Photons}/s}{\text{mrad}^2 \cdot \text{mm}^2 \cdot 0.1\% \text{ bandwidth}}$$

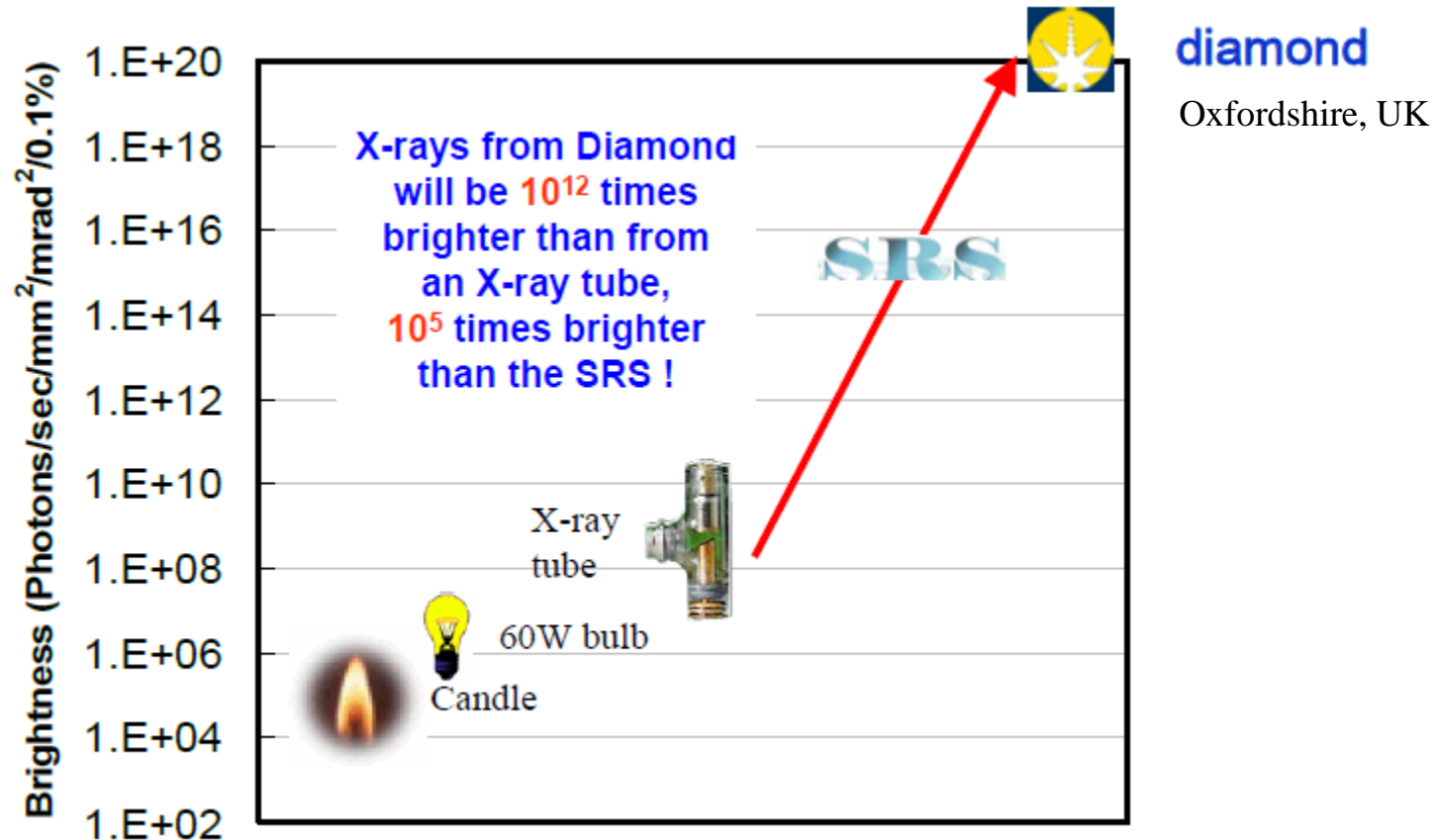


Brilliance is the figure of merit for the design of a new synchrotron source

Brilliance

Brilliance takes into account:

1. Number of photons produced per second
2. The angular divergence of the photons, or how fast the beam spreads out
3. The cross-section area of the beam
4. the photons falling within a bandwidth of 0.1% of the central wavelength or frequency

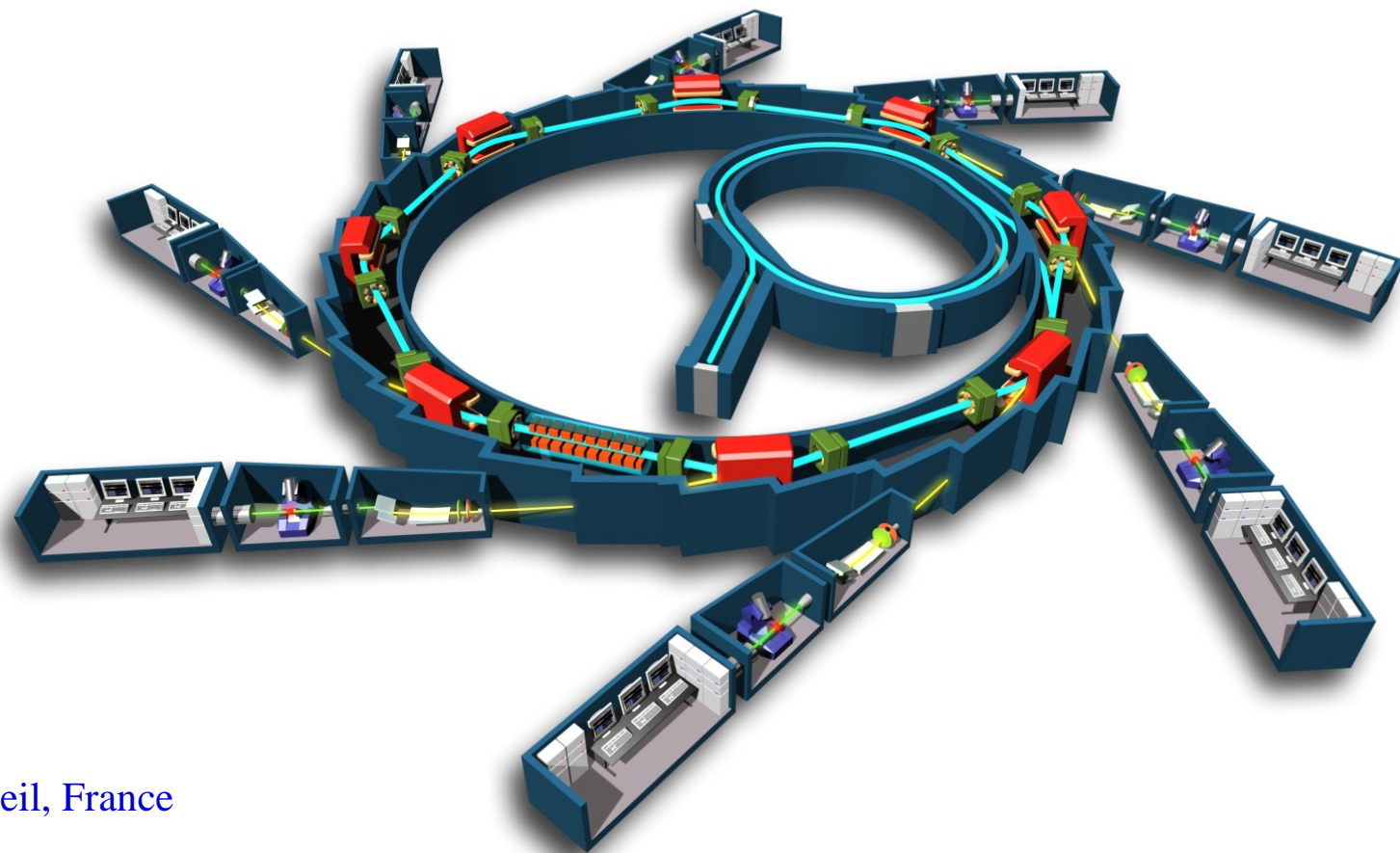


SRS = Synchrotron Radiation Source

Layout of a synchrotron radiation source

Electrons are generated and accelerated in a *LINAC*, further accelerated to the required energy in a *booster* and injected and stored in a *storage ring*.

The circulating electrons emit an intense beam of synchrotron radiation which is sent down the beamlines.



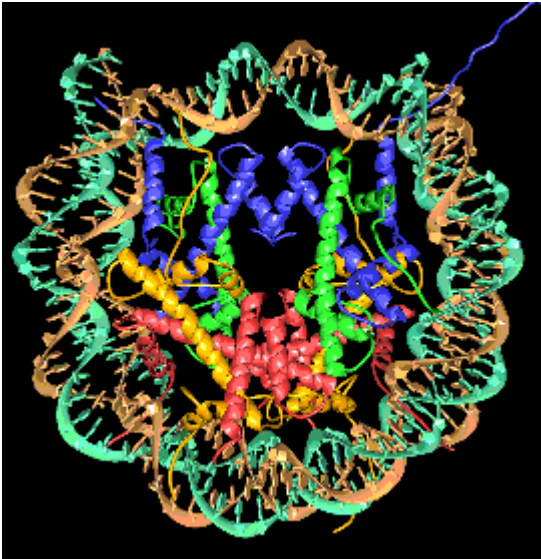
Soleil, France

Applications

Medicine, Biology, Chemistry, Material Science, Environmental Science and more

Biology

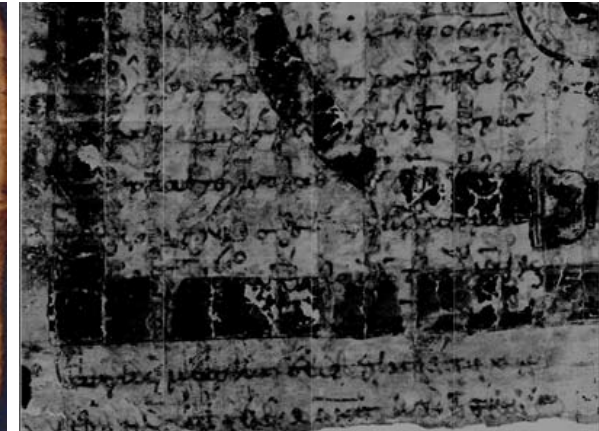
Reconstruction of the 3D structure of a nucleosome with a resolution of 0.2 nm



The collection of precise information on the molecular structure of chromosomes and their components can improve the knowledge of how the genetic code of DNA is maintained and reproduced

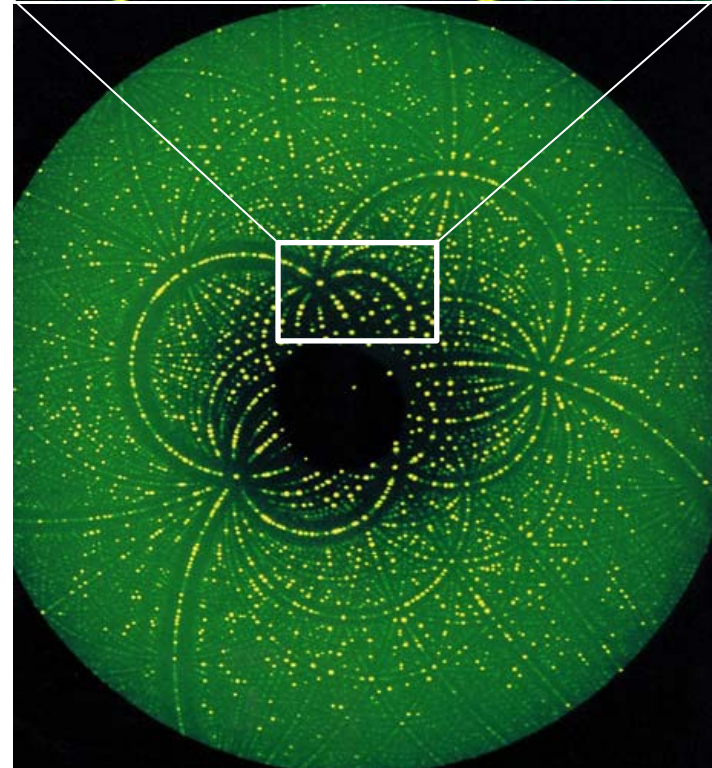
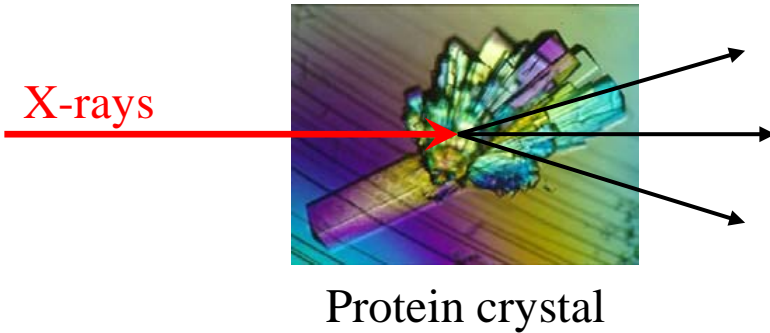
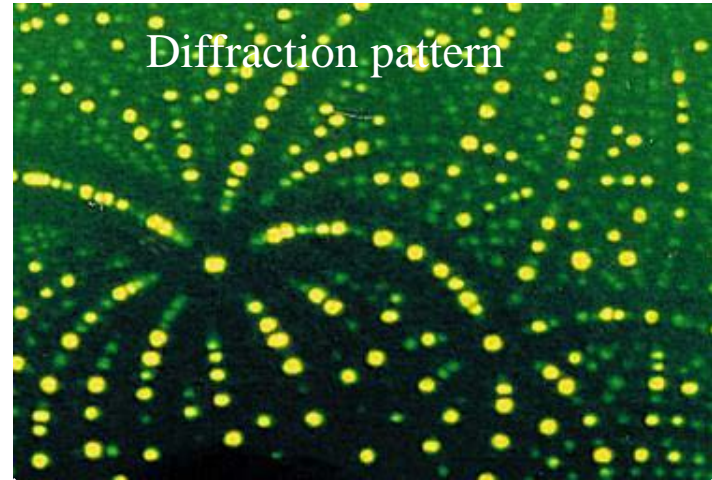
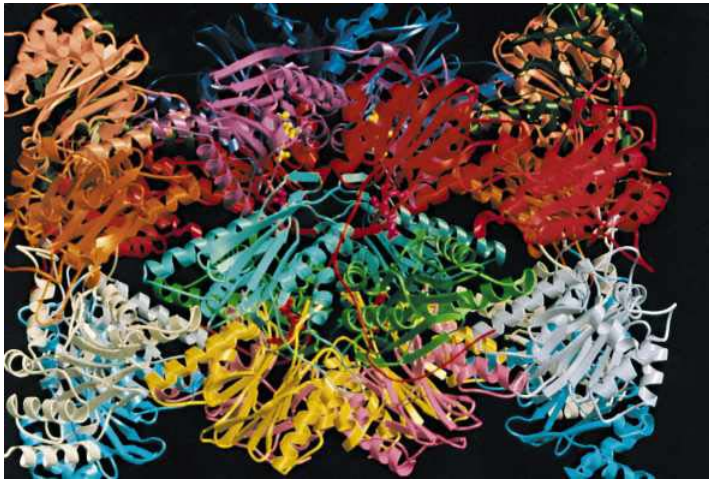
Archeology

A synchrotron X-ray beam at the SSRL facility illuminated an obscured work erased, written over and even painted over of the ancient mathematical genius Archimedes 287 B.C.

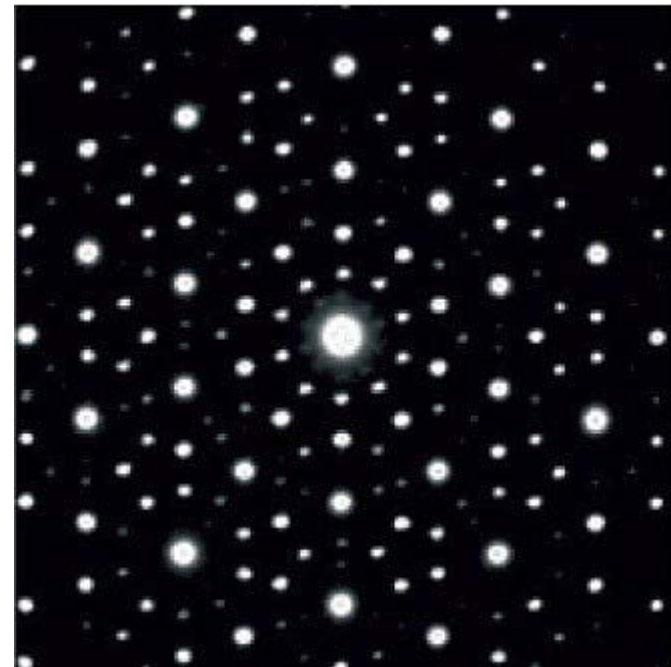
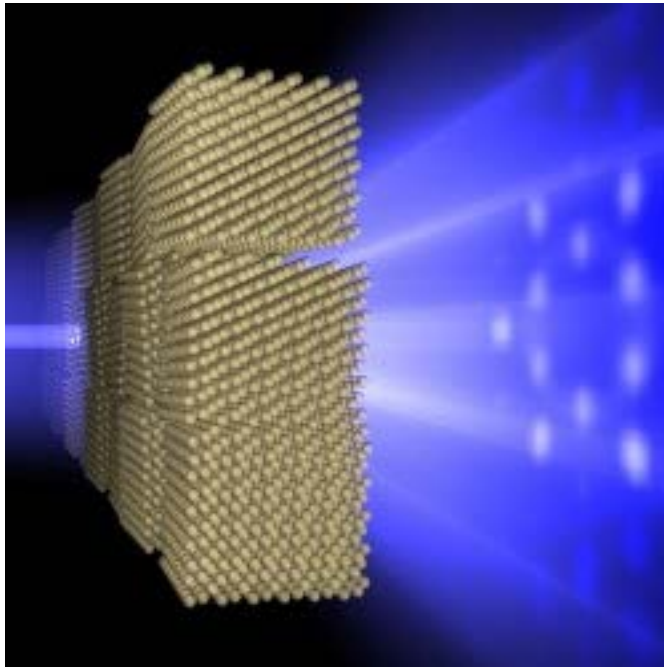


X-ray fluorescence imaging revealed the hidden text by revealing the iron contained in the ink used by a 10th century scribe. This X-ray image shows the lower left corner of the page.

Protein Crystallography



Bragg Scattering in Crystals

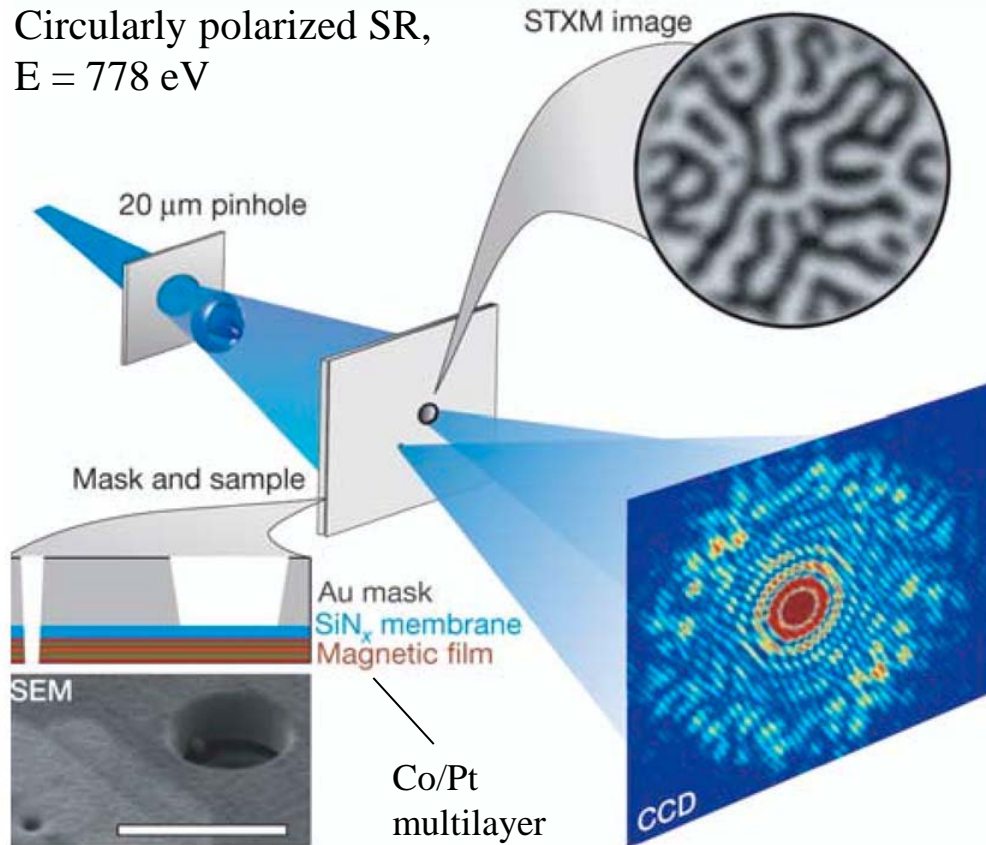


- ❖ Regular structure (crystal)
- ❖ Monochromatic light

⇒ Diffractive Pattern

Imaging of magnetic domains

Circularly polarized SR,
 $E = 778 \text{ eV}$



Lensless imaging of magnetic nanostructures by X-ray spectro-holography

S. Eisebitt¹, J. Lüning², W. F. Schlotter^{2,3}, M. Lürjen¹, O. Hellwig^{1,4},
W. Eberhardt¹ & J. Stöhr²

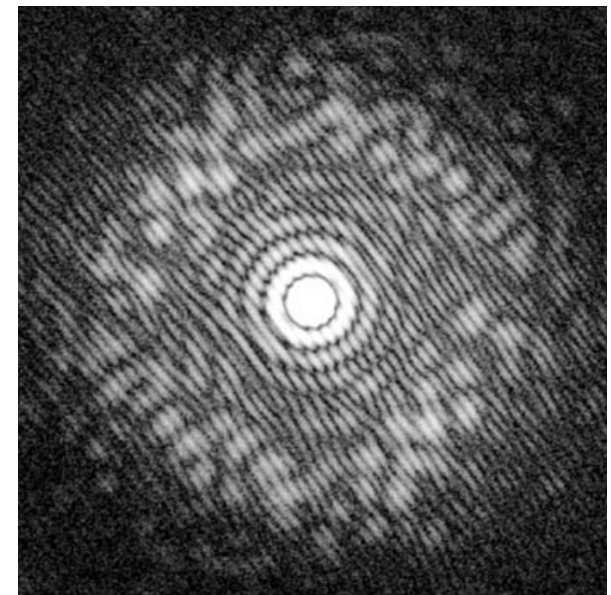
¹BESSY mbH, Albert-Einstein-Straße 15, 12489 Berlin, Germany

²SSRL, Stanford Linear Accelerator Center, 2575 Sand Hill Road, Menlo Park, California 94025, USA

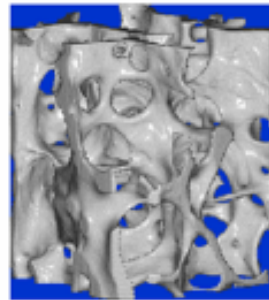
³Department of Applied Physics, 316 Via Pueblo Mall, Stanford University, Stanford, California 94305-4090, USA

⁴San Jose Research Center, Hitachi Global Storage Technologies, 650 Harry Road, San Jose, California 95120, USA

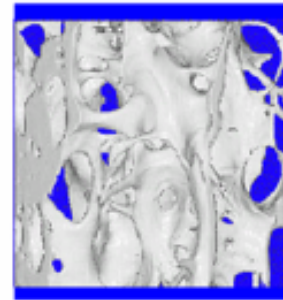
Nature 432, 885 (2004)



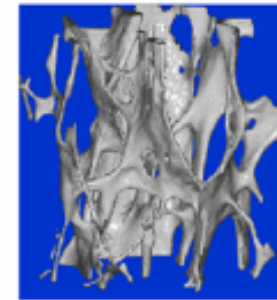
Microstructure of bones: Development during Osteoporosis disease



33 years

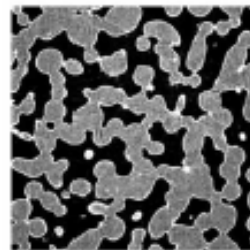


55 years

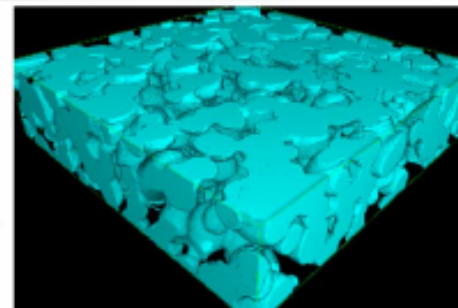
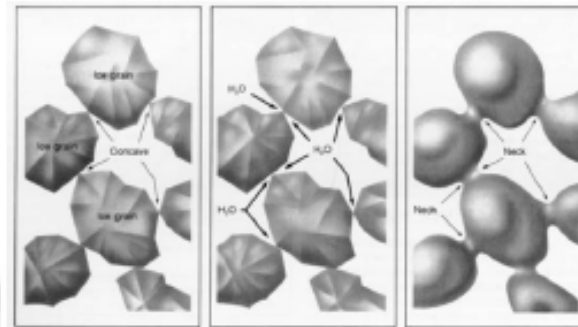


63 years

Microstructure of ice crystals in snow



1 mm



Structure of wet snow

Improvement of:

Spatial resolution

Energy resolution

Time resolution

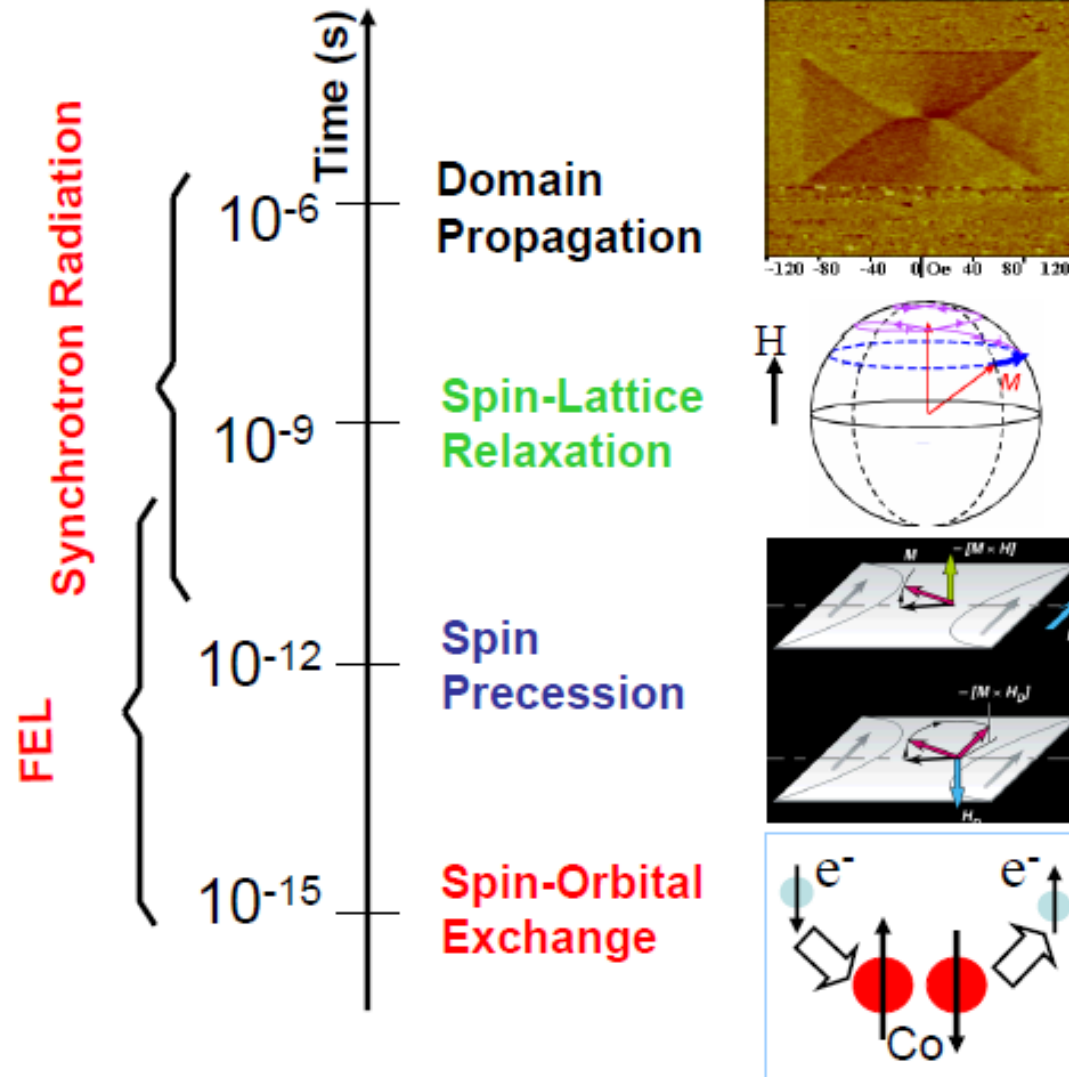
Most of present-day experiments are dealing with equilibrium properties of condensed matter. In the future, non-equilibrium properties will be of great interest:

Dynamics of phase transitions, magnetic switching phenomena, chemical reactions etc.

Reveal the underlying mechanisms by taking snapshots on ultrashort time scales!

Future experiments with Synchrotron Radiation

Time Scales in Magnetism



Limits of Storage – Ring Based Sources

Beam properties reflect the equilibrium

Dynamics of particle in the ring, resulting from averaging over all revolutions

Particles are re-cycled

Development of New Radiation Sources

Radiation is generated by single bunches passing through an undulator

Energy – Recovery Linear Accelerator (ERL)

Sub-Picosecond Pulsed Sources (SPPS)

X-ray Free Electron Laser (XFEL)

Limits of Storage – Ring Based Sources

Beam properties reflect the equilibrium

Dynamics of particle in the ring, resulting from averaging over all revolutions

Particles are re-cycled

Development of New Radiation Sources

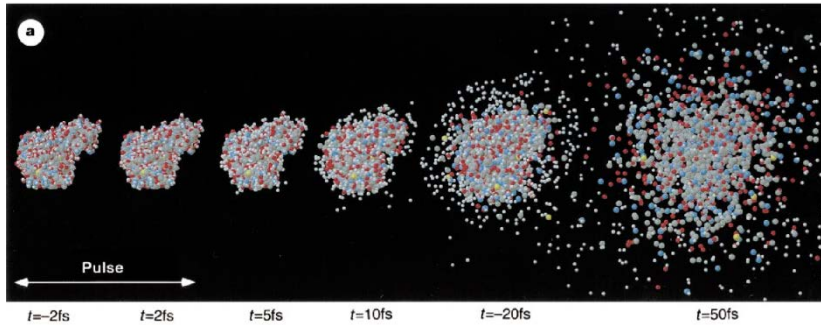
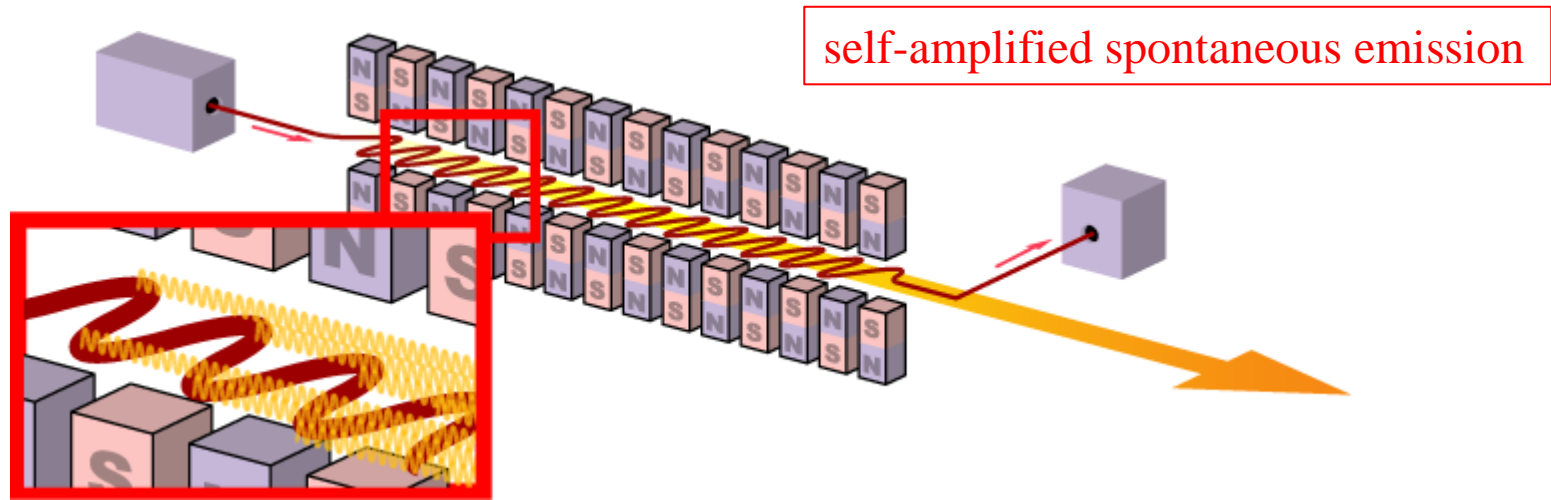
Radiation is generated by single bunches passing through an undulator

Energy – Recovery Linear Accelerator (ERL)

Sub-Picosecond Pulsed Sources (SPPS)

X-ray Free Electron Laser (XFEL)

X-ray free electron laser



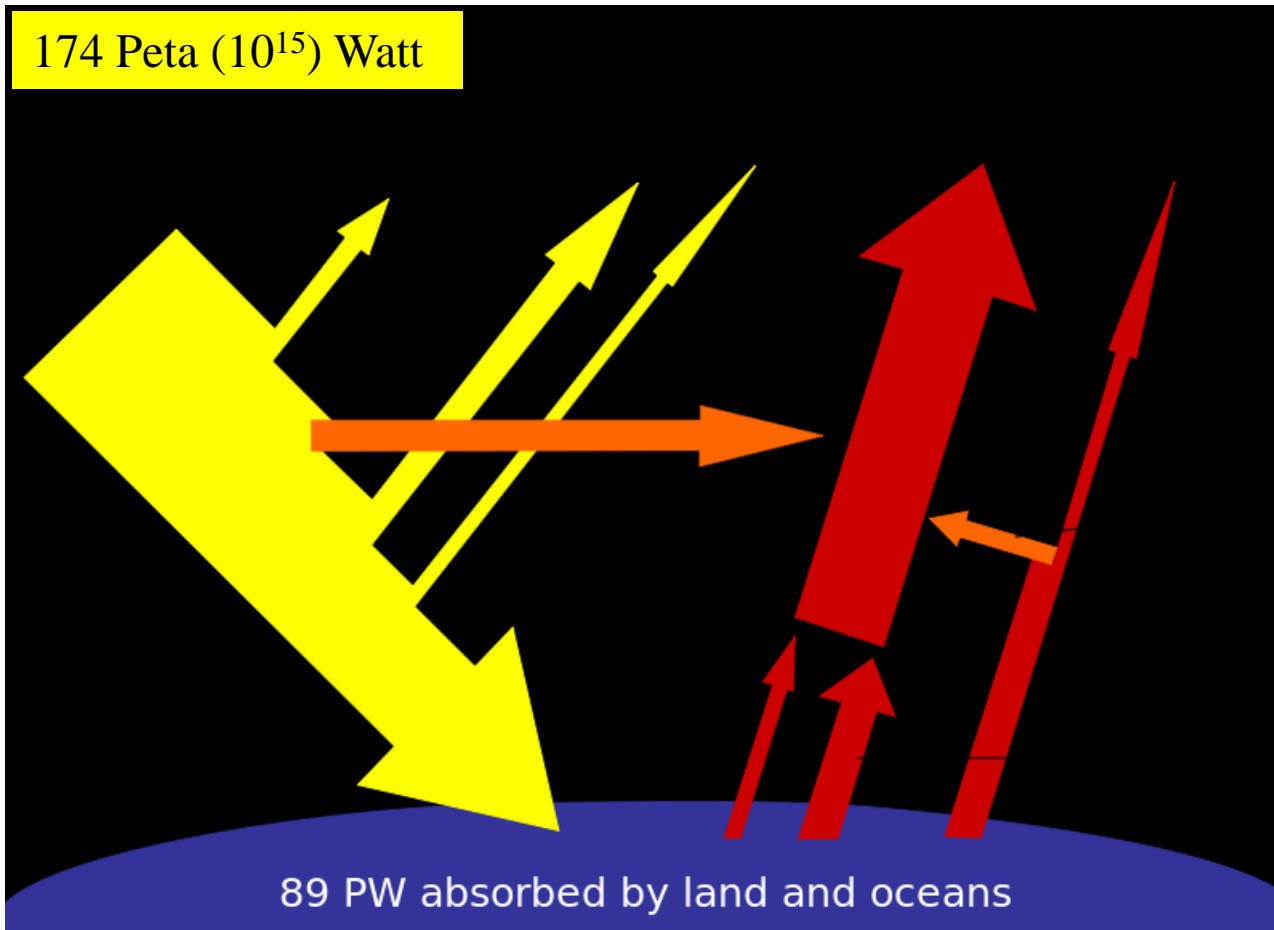
Explosion of a biomolecule (T4 lysozyme) after exposure to a 2-fs XFEL pulse ($E=12\text{ keV}$)



Desy XFEL



Total power received by Earth from the Sun

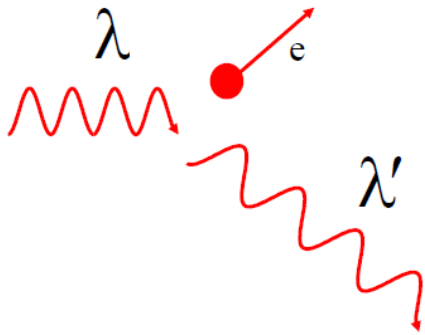


10 PW

@  eli
Nuclear Physics

extreme light infrastructure, Europe

Compton scattering and inverse Compton scattering



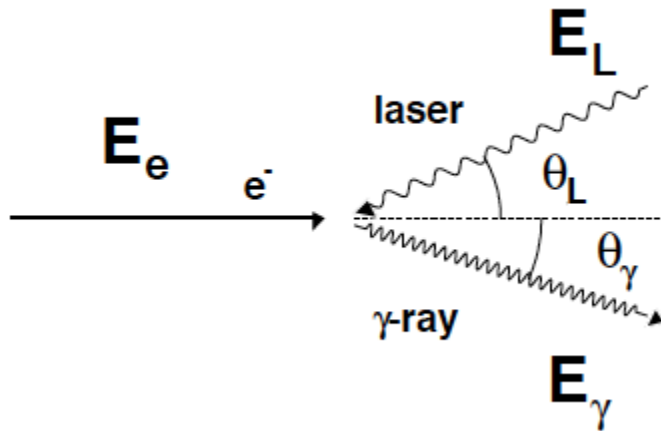
Compton scattering:

- Elastic scattering of a high-energy γ -ray on a free electron.
- **A fraction of the γ -ray energy is transferred to the electron.**
- The wave length of the scattered γ -ray is increased: $\lambda' > \lambda$.

$$h\nu \geq m_e c^2$$

$$\lambda' - \lambda = \frac{h}{m_e c} \cdot (1 - \cos\theta_\gamma)$$

$$E'_\gamma = \frac{E_\gamma}{1 + \frac{E_\gamma}{m_e c^2} \cdot (1 - \cos\theta)}$$



Inverse Compton scattering:

- Scattering of low energy photons on ultra-relativistic electrons.
- **Kinetic energy is transferred from the electron to the photon.**
- The wave length of the scattered γ -ray is decreased: $\lambda' < \lambda$.

$$\lambda' \approx \lambda \cdot \frac{1 - \beta \cdot \cos\theta_\gamma}{1 + \beta \cdot \cos\theta_L}$$

Inverse Compton scattering

- ❖ Electron is moving at relativistic velocity
- ❖ Transformation from **laboratory frame** to **reference frame of e^-** (rest frame):
in order to repeat the derivation for Compton scattering

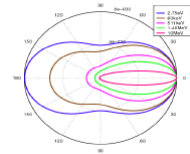
$$E_\gamma = \gamma \cdot E_\gamma \cdot \underbrace{\left(1 - \frac{v}{c} \cos\theta_{e-\gamma}\right)}_{\text{Doppler shift}}$$

$$\text{Lorentz factor: } \gamma = (1 - \beta^2)^{-1/2} = 1 + \frac{T_e^{\text{MeV}}}{931.5 \cdot 0.00055}$$

$$E'_\gamma = \frac{E_\gamma}{1 + \frac{E_\gamma}{m_e c^2} \cdot (1 - \cos\phi)}$$

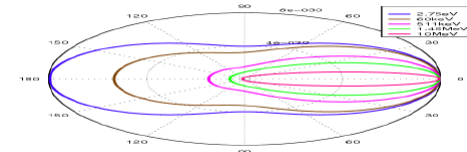
Compton scattering in rest frame of e^-

differential cross section (Klein-Nishina)



$$E'_\gamma = \gamma \cdot E'_\gamma \left(1 + \frac{v}{c} \cos\theta_{e-\gamma'}\right)$$

transformation into the laboratory frame



- ❖ **Limit** $E_\gamma \ll m_e c^2$

$$E'_\gamma \approx \gamma^2 \cdot E_\gamma \left(1 - \frac{v}{c} \cos\theta_{e-\gamma}\right) \left(1 + \frac{v}{c} \cos\theta_{e-\gamma'}\right)$$

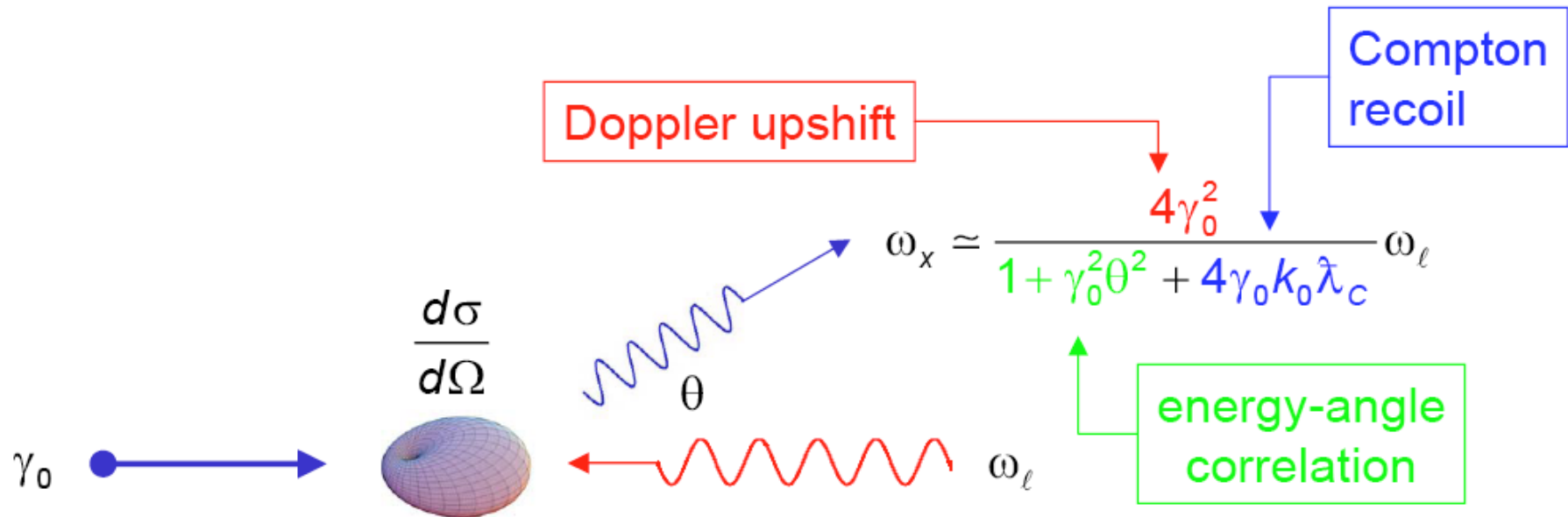
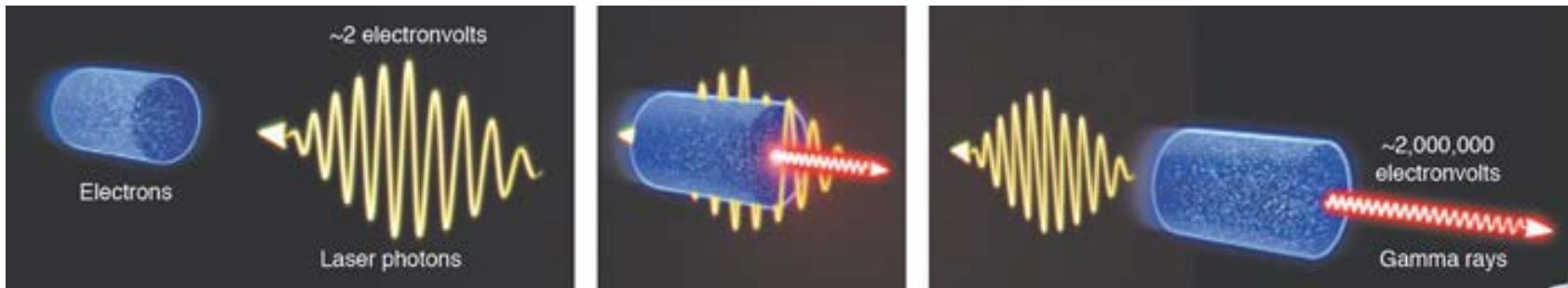
$$E'_\gamma \approx 4\gamma^2 \cdot E_\gamma$$



electron and γ interaction $\theta_{e-\gamma} \sim 180^\circ$

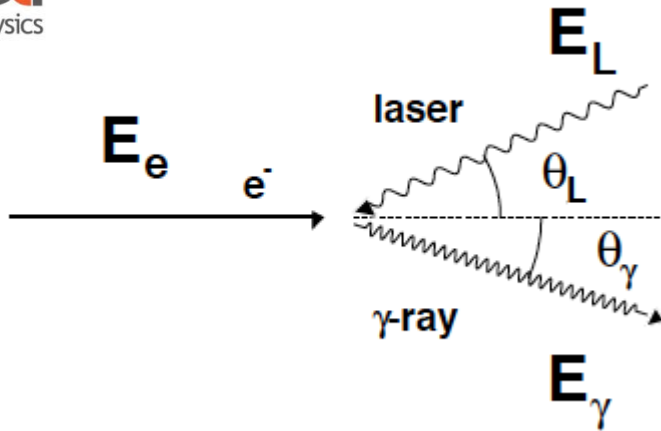
γ' emission relative to electron $\theta_{e-\gamma'} \sim 0^\circ$

Laser Compton backscattering



Energy – momentum conservation yields $\sim 4\gamma^2$ Doppler upshift
 Thomsons scattering cross section is very small ($6 \cdot 10^{-25} \text{ cm}^2$)
 ⇒ High photon and electron density are required

Gamma rays resulting after inverse Compton scattering



photon scattering on relativistic electrons ($\gamma \gg 1$)

$$h\nu = 2.3 \text{ eV} \quad (\equiv 515 \text{ nm})$$

$$T_e^{lab} = 720 \text{ MeV} \rightarrow \gamma_e = 1 + \frac{T_e^{lab} [\text{MeV}]}{931.5 \cdot A_e [\text{u}]} = 1410$$

$$E_\gamma = 2\gamma_e^2 \frac{1 + \cos\theta_L}{1 + (\gamma_e\theta_\gamma)^2 + a_0^2 + \frac{4\gamma_e E_L}{mc^2}} \cdot E_L$$

$$\frac{4\gamma_e E_L}{mc^2} = \text{recoil parameter}$$

$$a_L = \frac{eE}{m\omega_L c} = \text{normalized potential vector of the laser field}$$

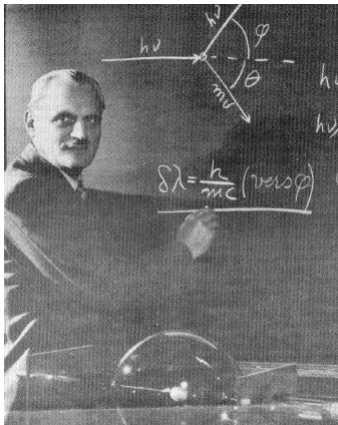
$$E = \text{laser electric field strength} \quad E_L = \hbar\omega_L$$

$$\gamma_e = \frac{E_e}{mc^2} = \frac{1}{\sqrt{1-\beta^2}} = \text{Lorentz factor}$$

maximum frequency amplification:

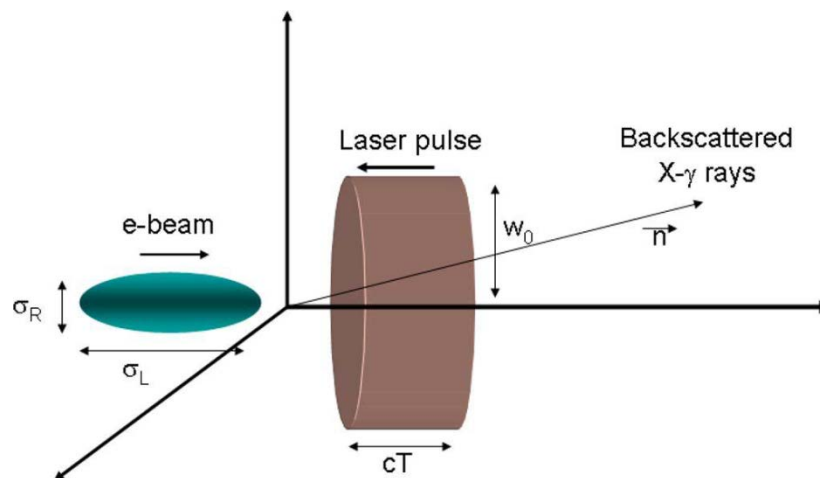
head-on collision ($\theta_L = 0^\circ$) & backscattering ($\theta_\gamma = 0^\circ$)

$$E_\gamma \sim 4\gamma_e^2 \cdot E_L \quad \cong 18.3 \text{ MeV}$$



A. H. Compton
Nobel Prize 1927

Scattered photons in collision



Yb: Yag J-class laser
10 Peta (10^{15}) Watt

$Q = 1[nC]$ $U_L = 0.5[J]$ $h\nu_L = 2.4[eV] = 3.86 \cdot 10^{-19}[J] \cong 515[nm]$
 $\rightarrow N_e = 6.25 \cdot 10^9$ $\rightarrow N_L = 1.3 \cdot 10^{18}$

Luminosity: $L = \frac{N_L \cdot N_e}{4\pi \cdot \sigma_R^2} \cdot f \cong 2.9 \cdot 10^{32} \cdot f [cm^{-2}s^{-1}]$ $\sigma_R = 15[\mu m]$

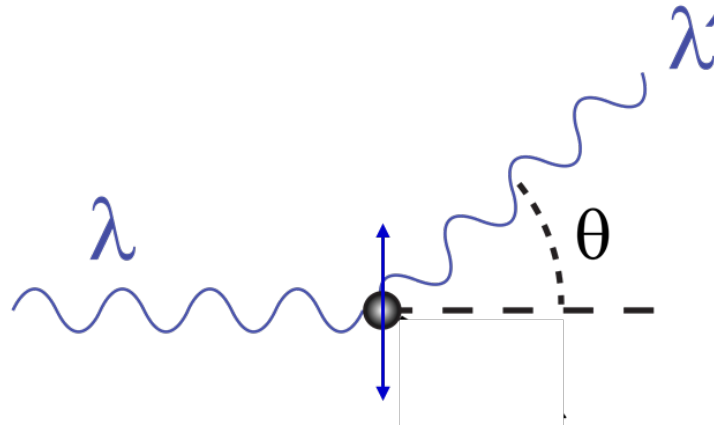
γ -ray rate: $N_\gamma = L \cdot \sigma_{Thomson} \cong 2 \cdot 10^8 \cdot f [s^{-1}]$ $\sigma_T = 0.67 \cdot 10^{-24}[cm^2]$
 (full spectrum)

repetition rate:
 $f = 3.2 kHz$

Thomson Scattering



J. J. Thomson
Nobel prize 1906



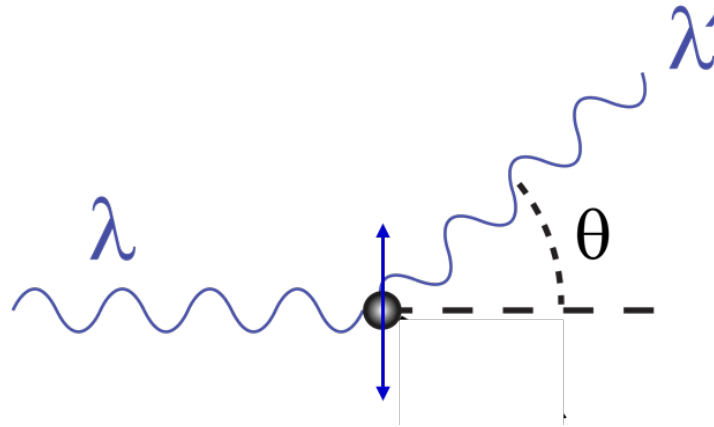
Thomson scattering = elastic scattering of electromagnetic radiation by an electron at rest

- the electric and magnetic components of the incident wave act on the electron
- the electron acceleration is mainly due to the electric field
 - the electron will move in the direction of the oscillating electric field
 - the moving electron will radiate electromagnetic dipole radiation
 - the radiation is emitted mostly in a direction perpendicular to the motion of the electron
 - the radiation will be polarized in a direction along the electron motion

Thomson Scattering



J. J. Thomson
Nobel prize 1906



$$\frac{d\sigma_T(\theta)}{d\Omega} = \frac{1}{2}r_0^2 \cdot (1 + \cos^2\theta)$$

differential cross section

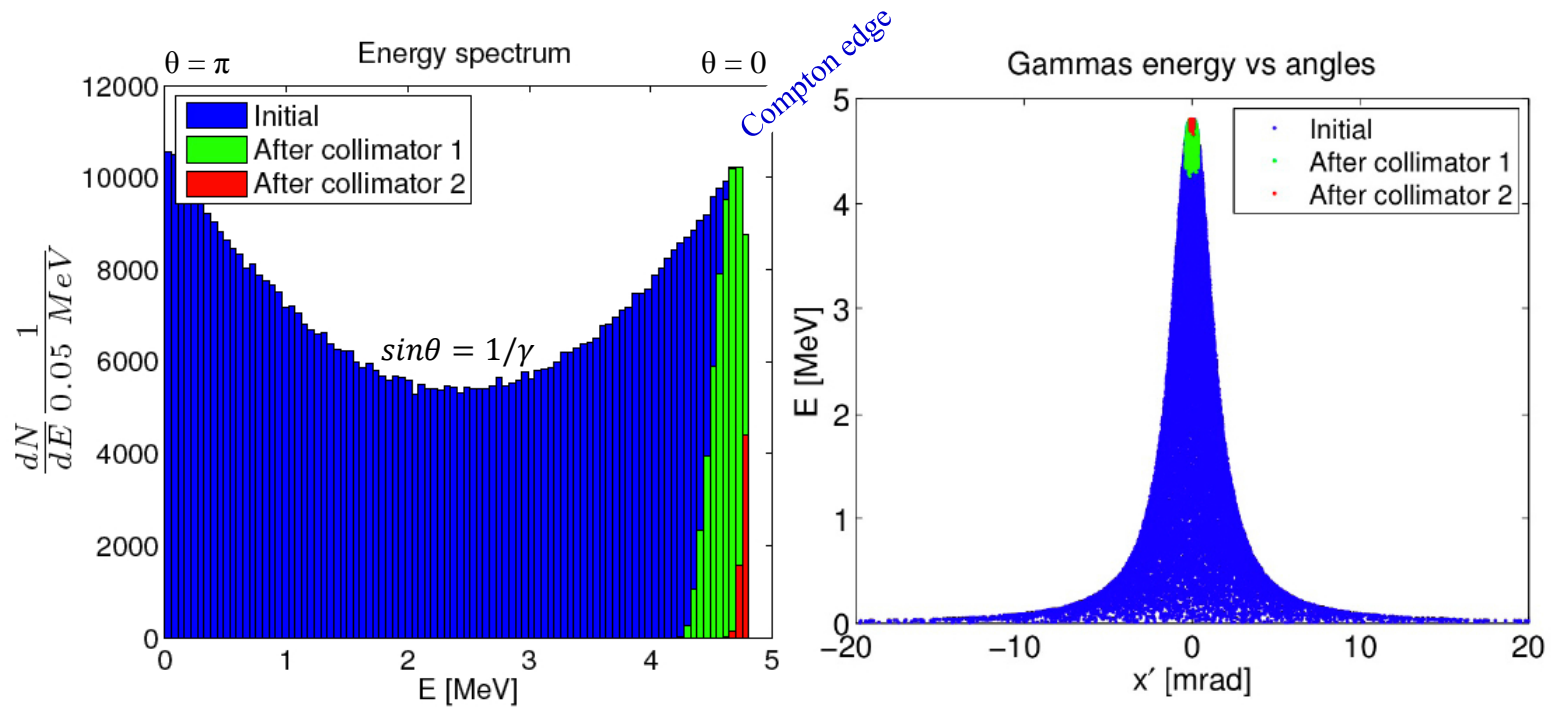
$$r_0 = \frac{e^2}{4\pi\epsilon_0 m_e c^2} = 2.818 \cdot 10^{-15} [m]$$

classical electron radius

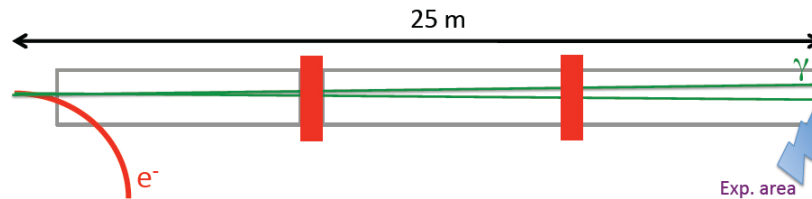
$$\sigma_T = \int \frac{d\sigma_T(\theta)}{d\Omega} d\Omega = \frac{2\pi r_0^2}{2} \int_0^\pi (1 + \cos^2\theta) d\theta = \frac{8\pi}{3} r_0^2 = 6.65 \cdot 10^{-29} [m^2] = 0.665 [b]$$

Scattered photons in collision

$$E_\gamma = 2\gamma_e^2 \frac{1 + \cos\theta_L}{1 + (\gamma_e\theta_\gamma)^2 + a_0^2 + \frac{4\gamma_e E_L}{mc^2}} \cdot E_L$$

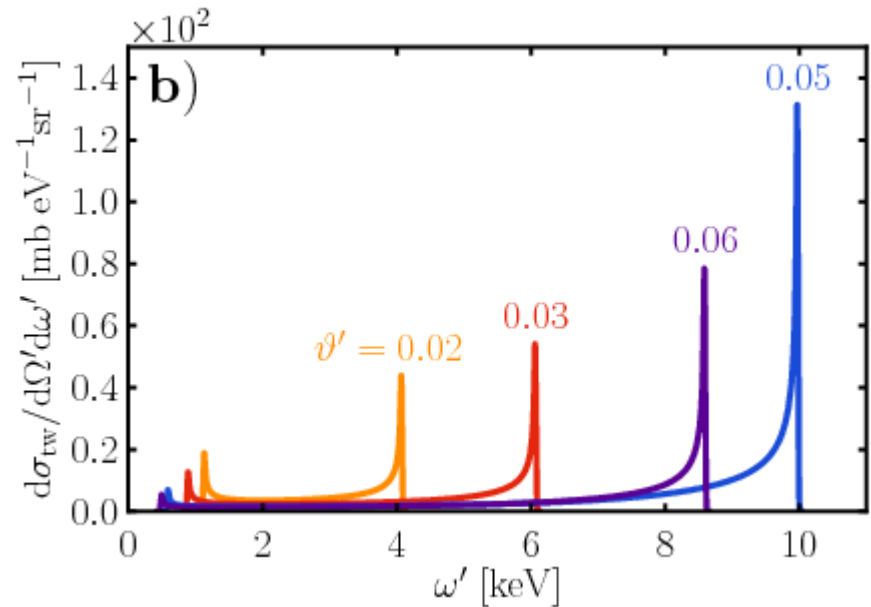
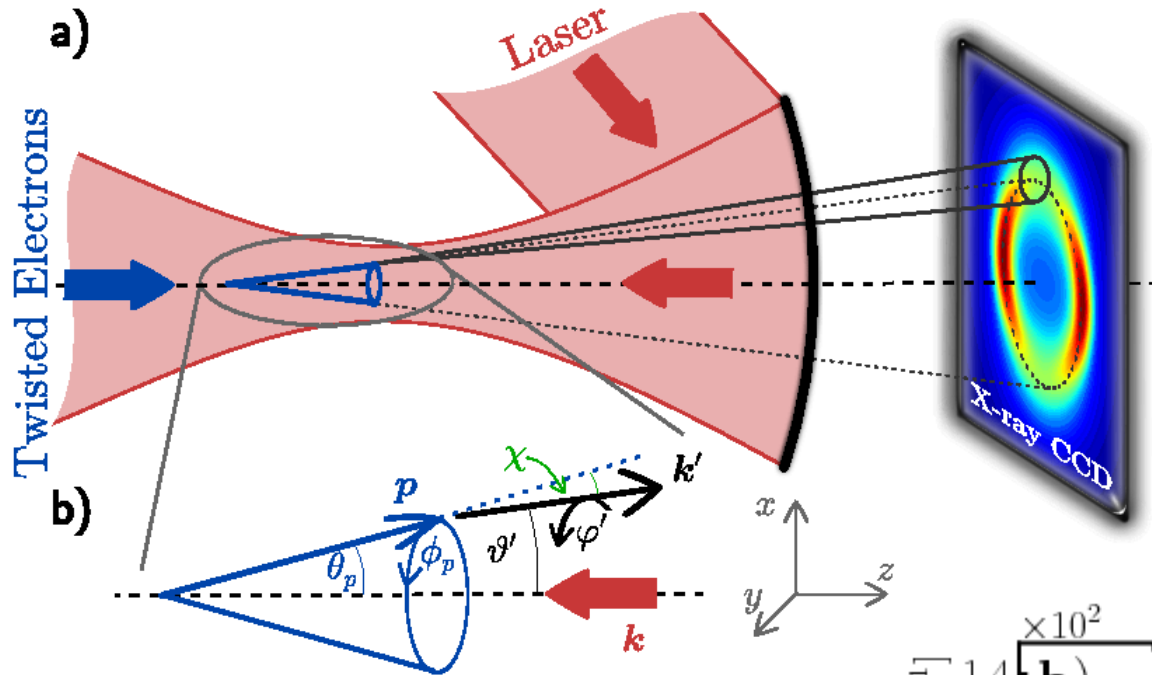


Photon extraction line

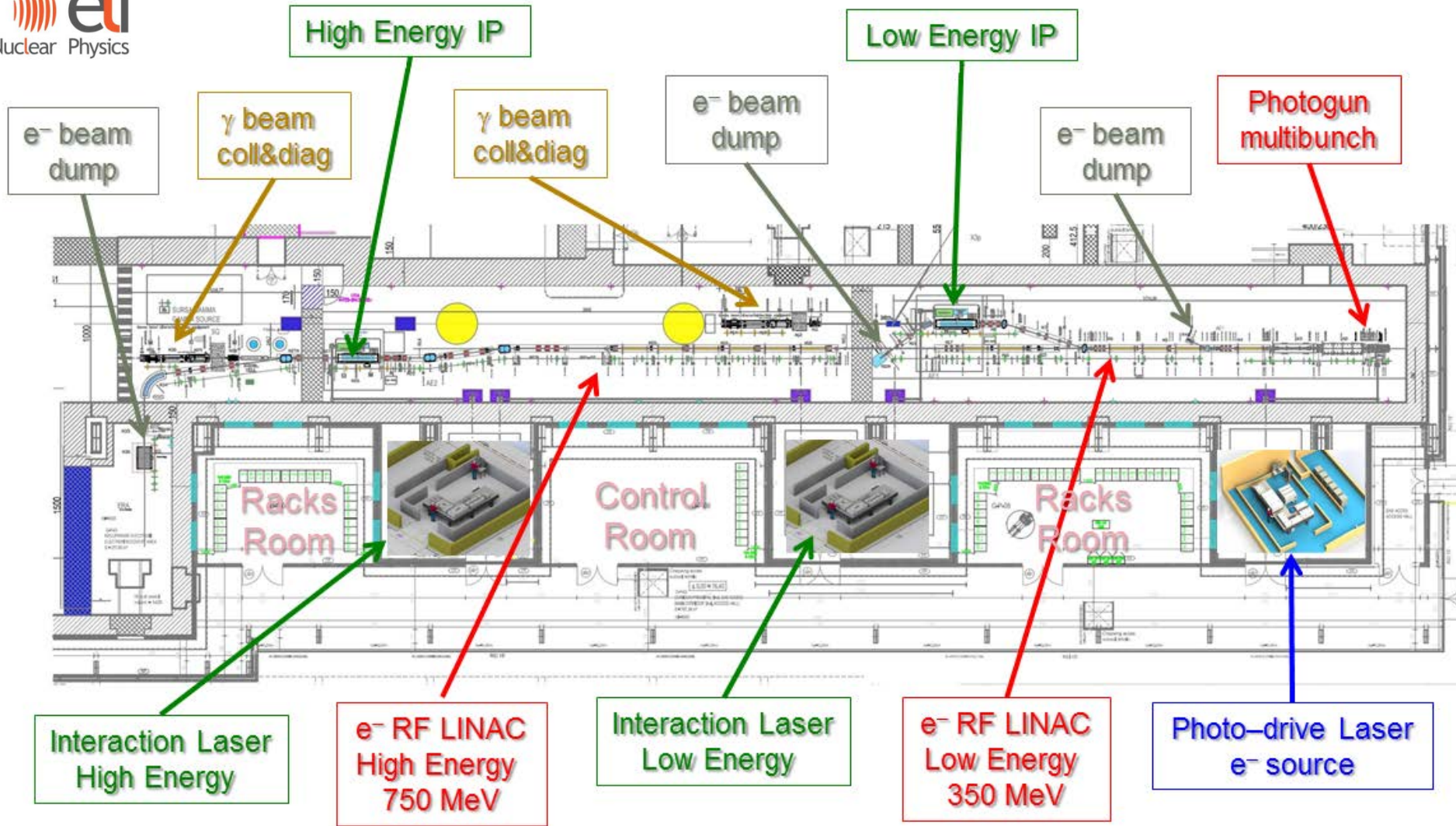


- Collimator 1 : d=11 m r= 0.3 cm , t= 5 cm (W)
- Collimator 2 : d=15 m r= 0.1 cm , t= 5 cm (W)

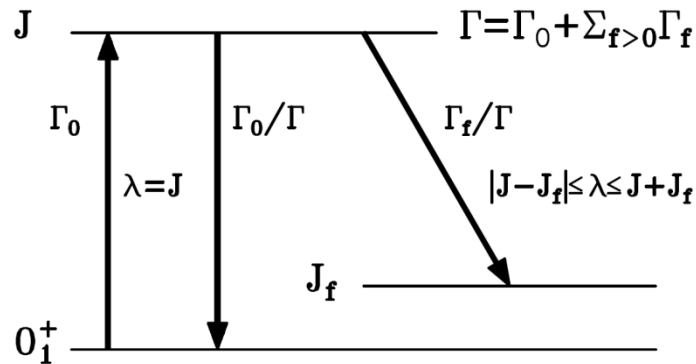
Inverse Compton scattering of laser light



Extreme Light Infrastructure – Nuclear Physics



Nuclear Resonance Fluorescence



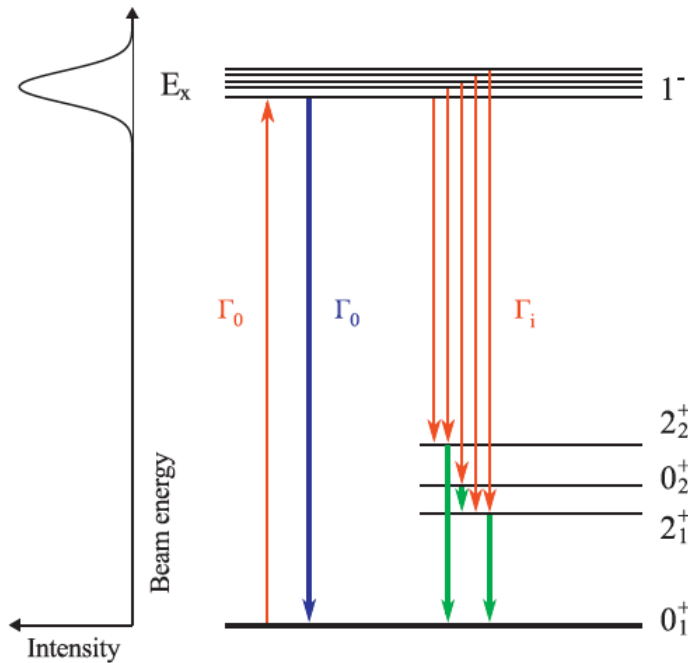
- Widths of particle-bound states: $\Gamma \leq 10eV$

- Breit-Wigner absorption resonance curve for isolated resonance:

$$\sigma_a(E) = \pi \bar{\lambda}^2 \frac{2J + 1}{2} \frac{\Gamma_0 \Gamma}{(E - E_r)^2 + (\Gamma/2)^2} \sim \Gamma_0/\Gamma$$

- Resonance cross section can be very large: $\sigma_0 \cong 200 [b]$ (for $\Gamma_0 = \Gamma, 5 \text{ MeV}$)
- Example: 10 mg, $A \sim 200 \rightarrow N_{\text{target}} = 3 \cdot 10^{19}, N_\gamma = 100, \text{ event rate} = 0.6 [\text{s}^{-1}]$

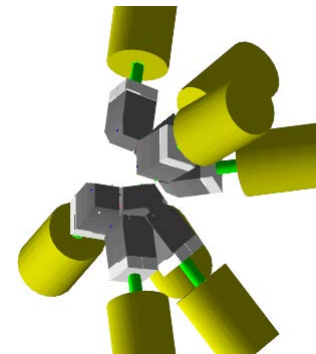
Nuclear Resonance Fluorescence



Count rate estimate

- $10^4 \gamma/(s \text{ eV})$ in 100 macro pulses
- $100 \gamma/(s \text{ eV})$ per macro pulse
- example: 10 mg, $A \sim 200$ target
- resonance width $\Gamma = 1 \text{ eV}$
- 2 excitations per macro pulse
- 0.6 photons per macro pulse in detector
- pp-count rate 6 Hz
- 1000 counts per 3 min

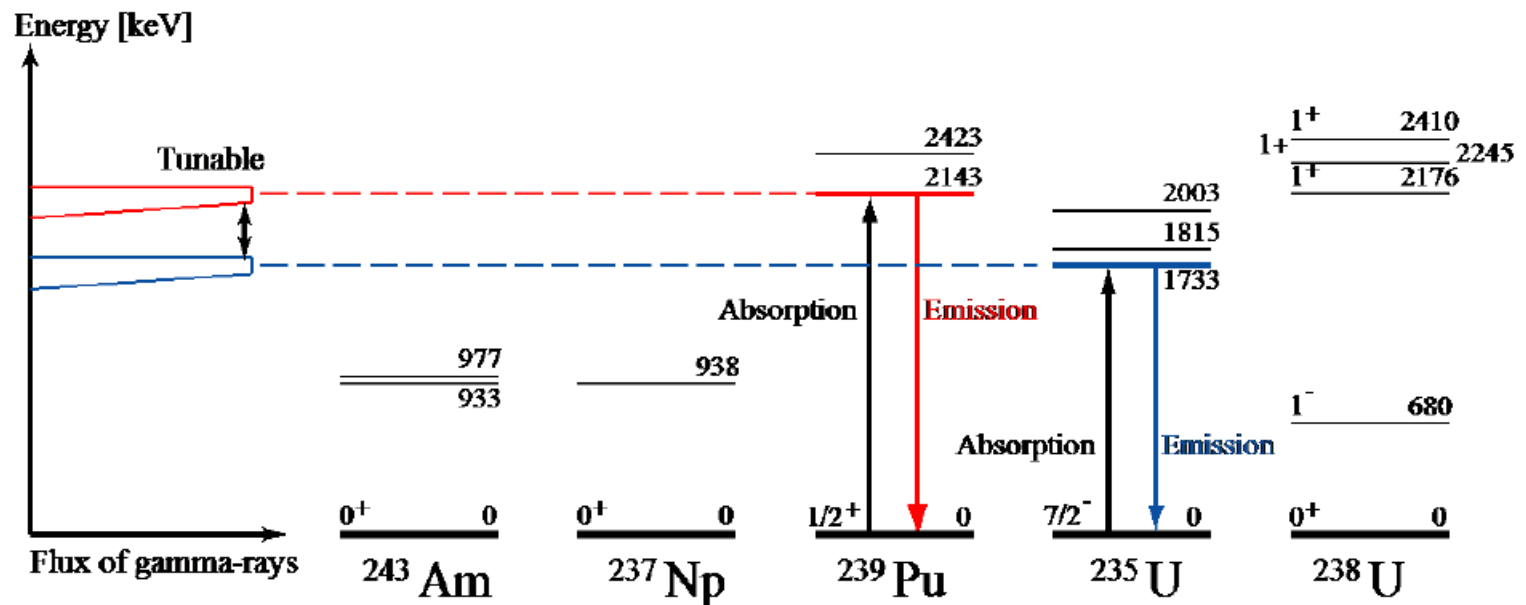
❖ narrow band width 0.5%



8 HPGe detectors
2 rings at 90° and 127°
 $\epsilon_{\text{rel}}(\text{HPGe}) = 100\%$
solid angle $\sim 1\%$
photopeak $\epsilon_{\text{pp}} \sim 3\%$

Nuclear Resonance Fluorescence

- ❖ narrow bandwidth allows selective excitation and detection of decay channels



Deformation and Scissors Mode

❖ Decay to intrinsic excitations

